NAVAL POSTGRADUATE SCHOOL

MONTEREY, CALIFORNIA

THESIS

ANALYSIS OF THE PERFORMANCE OF AN OPTIMIZATION MODEL FOR TIME-SHIFTABLE ELECTRICAL LOAD SCHEDULING UNDER UNCERTAINTY

by

John A. Olabode

December 2016

Thesis Co-Advisors:	Susan M. Sanchez
	Emily M. Craparo
Second Reader:	W. Matthew Carlyle

THIS PAGE INTENTIONALLY LEFT BLANK

REPORT DOCUMENTATION PAGE			Form Approved OMB No. 0704–0188

1. AGENCY USE ONLY *(Leave Blank)*	2. REPORT DATE	3. REPORT TYPE AND DATES COVERED
	December 2016	Master's Thesis 01-04-2016 to 09-23-2016

4. TITLE AND SUBTITLE

ANALYSIS OF THE PERFORMANCE OF AN OPTIMIZATION MODEL FOR TIME-SHIFTABLE ELECTRICAL LOAD SCHEDULING UNDER UNCERTAINTY

5. FUNDING NUMBERS

6. AUTHOR(S)

John A. Olabode

7. PERFORMING ORGANIZATION NAME(S) AND ADDRESS(ES)

Naval Postgraduate School
Monterey, CA 93943

8. PERFORMING ORGANIZATION REPORT NUMBER

9. SPONSORING / MONITORING AGENCY NAME(S) AND ADDRESS(ES)

N/A

10. SPONSORING / MONITORING AGENCY REPORT NUMBER

11. SUPPLEMENTARY NOTES

The views expressed in this document are those of the author and do not reflect the official policy or position of the Department of Defense or the U.S. Government. IRB Protocol Number: N/A.

12a. DISTRIBUTION / AVAILABILITY STATEMENT

Approved for public release. Distribution is unlimited.

12b. DISTRIBUTION CODE

13. ABSTRACT *(maximum 200 words)*

To ensure sufficient capacity to handle unexpected demands for electric power, decision makers often over-estimate expeditionary power requirements. Therefore, we often use limited resources inefficiently by purchasing more generators and investing in more renewable energy sources than needed to run power systems on the battlefield.

Improvement of the efficiency of expeditionary power units requires better managing of load requirements on the power grids and, where possible, shifting those loads to a more economical time of day. We analyze the performance of a previously developed optimization model for scheduling time-shiftable electrical loads in an expeditionary power grids model in two experiments. One experiment uses model data similar to the original baseline data, in which expected demand and expected renewable production remain constant throughout the day. The second experiment introduces unscheduled demand and realistic fluctuations in the power production and the demand distributions data that more closely reflect actual data.

Our major findings show energy grid power production composition affects which uncertain factor(s) influence fuel consumption, and uncertainty in the energy grid system does not always increase fuel consumption by a large amount. We also discover that the generators running the most do not always have the best load factor on the grid, even when optimally scheduled.

14. SUBJECT TERMS

expeditionary, energy, optimization, robust optimization, Parameter Uncertainty, deferrable, fuel, mixed integer linear program, design of experiment, Latin hypercube, fuel consumption, robust designs

15. NUMBER OF PAGES 93

16. PRICE CODE

17. SECURITY CLASSIFICATION OF REPORT	18. SECURITY CLASSIFICATION OF THIS PAGE	19. SECURITY CLASSIFICATION OF ABSTRACT	20. LIMITATION OF ABSTRACT
Unclassified	Unclassified	Unclassified	UU

NSN 7540-01-280-5500 — Standard Form 298 (Rev. 2–89) Prescribed by ANSI Std. 239–18

THIS PAGE INTENTIONALLY LEFT BLANK

Approved for public release. Distribution is unlimited.

ANALYSIS OF THE PERFORMANCE OF AN OPTIMIZATION MODEL FOR TIME-SHIFTABLE ELECTRICAL LOAD SCHEDULING UNDER UNCERTAINTY

John A. Olabode
Lieutenant Commander, United States Navy
B.S., University of Ibadan, Nigeria, 1999

Submitted in partial fulfillment of the
requirements for the degree of

MASTER OF SCIENCE IN OPERATIONS RESEARCH

from the

NAVAL POSTGRADUATE SCHOOL
December 2016

Approved by: Susan M. Sanchez
Thesis Co-Advisor

Emily M. Craparo
Thesis Co-Advisor

W. Matthew Carlyle
Second Reader

Patricia A. Jacobs
Chair, Department of Operations Research

THIS PAGE INTENTIONALLY LEFT BLANK

ABSTRACT

To ensure sufficient capacity to handle unexpected demands for electric power, decision makers often over-estimate expeditionary power requirements. Therefore, we often use limited resources inefficiently by purchasing more generators and investing in more renewable energy sources than needed to run power systems on the battlefield.

Improvement of the efficiency of expeditionary power units requires better managing of load requirements on the power grids and, where possible, shifting those loads to a more economical time of day. We analyze the performance of a previously developed optimization model for scheduling time-shiftable electrical loads in an expeditionary power grids model in two experiments. One experiment uses model data similar to the original baseline data, in which expected demand and expected renewable production remain constant throughout the day. The second experiment introduces unscheduled demand and realistic fluctuations in the power production and the demand distributions data that more closely reflect actual data.

Our major findings show energy grid power production composition affects which uncertain factor(s) influence fuel consumption, and uncertainty in the energy grid system does not always increase fuel consumption by a large amount. We also discover that the generators running the most do not always have the best load factor on the grid, even when optimally scheduled.

THIS PAGE INTENTIONALLY LEFT BLANK

Table of Contents

List of Figures

THIS PAGE INTENTIONALLY LEFT BLANK

List of Tables

THIS PAGE INTENTIONALLY LEFT BLANK

List of Acronyms and Abbreviations

AMMPS Advanced Medium Mobile Power Sources

ANOVA analysis of variance

ASD Assistant Secretary of Defense

AVL AVL company fuel consumption measurement system

CENTCOM Central Command

COC chain of command

CSV Comma separated values

DCAC direct current air cooler

DOD Department of Defense

DOE design of experiment

DSM demand-side management

ECU environmental control unit

EMS Energy Management System

FOBs forward operating bases

FY fiscal year

FYDP Future Year Defense Plan

GAMS General Algebraic Modeling System

GREENS Ground Renewable Expeditionary Energy Network Systems

HEG Hybrid Electric Grid

HESM Hybrid Energy Storage Module

HTPS Hybrid Tactical Power System

HVAC heating ventilation and air conditioning

IEDs improvised explosive devices

IESMA Innovative Energy Solutions for Military Applications

kW kilowatt

kWh kilowatt hour

LGCY legacy system

MAGTF Marine Air-Ground Task Force

MASINT measurement and signature intelligence

MEAT Marine Energy Assessment Team

MEPGS Mobile Electric Power Generating Sources

MILP mixed integer linear program

MPEM MAGTF Power and Energy Model

NASA National Aeronautics and Space Administration

NOLH nearly orthogonal Latin hypercube

NPS Naval Postgraduate School

OEPP Operational Energy Plans and Programs

ONR Office of Naval Research

PDISE Power Distribution Illumination System Electrical

PM MEP Project Manager for Mobile Electric Power

REDUCE Renewable Energy for Distributed Under-Supplied Command Environment

RH-PFK rolling horizon with perfect future knowledge

RH-U rolling horizon with uncertainty

RO robust optimization

SEED Simulation Experiments and Efficient Designs

SO Stochastic optimization

SOFC solid oxide fuel cell

SOS2 Specially Ordered Set Type 2

SRWBR short range wide band radio

TCP Transmission Control Protocol

TQGs Tactical Quiet Generators

UAVs unmanned aerial vehicles

USMC U.S. Marine Corps

USN U.S. Navy

UDP User Datagram Protocol

USG United States government

THIS PAGE INTENTIONALLY LEFT BLANK

Executive Summary

Operational energy demand and requirements are major factors to consider in any military operation. The demand continues to grow as the U.S. military addresses conflicts across the globe and cooperates with other nations on humanitarian aid efforts. In fiscal year (FY) 2013, the Department of Defense (DOD) used more than 9 million barrels of liquid fuel to support Operation Enduring Freedom in Afghanistan [1]. To ensure an uninterrupted flow of electrical energy for these military missions, most of the expeditionary and other DOD forward operating bases (FOBs) rely on fossil fuel-based generators to power equipment and systems for military operations. Over estimated power requirements account for this high-energy demand, which often results in an inefficient power grid system.

Naval Postgraduate School Operations Research student John G. Sprague provides us with a tool to effectively manage load requirements in his thesis [2]. However, his model treats unmanaged load requirements and production as deterministic parameters. This thesis aims to investigate the impact of uncertain factors influencing fuel consumption and to obtain useful insights on the model's performance to support future development of a robust version of it.

We conduct a multifactor-designed experiment of key input parameters in Sprague's model to more fully understand contributions to fuel savings by running two experiments. In both experiments, we use a nearly orthogonal Latin hypercube (NOLH) design with 33 design points. The baseline for the first experiment is very similar to Sprague's baseline model but introduces systematic variation into six factors related to uncertainty in the system. In the second experiment, we seek additional insights into the model's behavior in situations where the renewable energy is a larger part of the energy production and the unscheduled demand varies during the day. We change the composition of the power grid by increasing the renewable energy production and also modify our expected unscheduled demand and expected renewable production data to reflect patterns that are more realistic in an expeditionary power grid system. We conduct our analysis of these two experiments using JMP Pro Version 12.0.1 [3].

Our analysis pinpoints the heat transfer intercept as the dominant uncertain factor contributing to the cumulative total fuel consumption. The heat transfer intercept represents the shelter's equilibrium heat transfer rate, which determines how fast heat is added to or removed from the shelter. Insights obtained from our study include the effect of the composition of the power grid's energy production on generator fuel consumption and the importance of properly matching the FOBs' power requirements with the generators' power ratings. Some notable findings include:

- In terms of fuel consumption, the first experiment illustrates that the rolling horizon with perfect future knowledge (RH-PFK) model variant always performs better than the rolling horizon with uncertainty (RH-U) by up to 8%. Also, the second experiment demonstrates that the RH-PFK performs better than the RH-U by up to 14%.
- It is possible to meet power demand requirements with fewer resources, such as the number of generators running simultaneously, and hence, less fuel consumption.
- The selection of the type and characteristics of shelters or structures to erect at the FOBs could play a key role in fuel consumption.
- The generator that runs most often does not always have the best load factor. The mixture of generator ratings available for power production on the power grid affects generator load factors and subsequent fuel consumption.

This study comes from a desire to improve U.S. military energy use on the battlefield. The cost associated with too much energy use goes beyond monetary resources; lives are lost, and the future capabilities budget is diminished. This thesis provides useful insights on how to reduce power grid energy consumption by using a powerful combination of an optimization model and design of experiment (DOE) analysis. Ultimately, the U.S. military expeditionary power grid system should be resilient and self-sustaining for our assigned missions around the world.

References

[1] S. Burke, "Statements submitted to the Subcommittee on Readiness and Management Support, Senate Armed Services Committee," Assistant Secretary of Defense for Operational Energy Plans and Programs, 2014.

[2] J. Sprague, "Optimal scheduling of time-shiftable electric loads in expeditionary power grids," Master's thesis, Operations Research Dept., Naval Postgraduate School, Monterey, CA, Sep. 2015.

[3] SAS Institute Inc., "JMP Pro version 12.0.1," Cary, NC, 1989-2007, 2016.

Acknowledgments

I would like to thank Professor Susan Sanchez and Professor Emily Craparo for their guidance, patience, inspiration and tireless coaching in getting this work completed. Their wisdom and expert advice were instrumental to my success.

I would also like to thank Professor Matthew Carlyle, who spent a lot of time going through my programming codes and reviewing the entire work. His critical review and discerning judgment were vital to the completion of this work.

The students, faculty and staff of the Operations Research Department at the Naval Postgraduate School deserve recognition, as well. Their professionalism, dedication to top-notch education, and commitment to national security issues motivated me throughout my study at NPS.

Finally, I owe everything to the almighty God, who has blessed me with the most wonderful family in the world. My wife, Tolulope, and our children, Victor and Victoria, have always supported me throughout my career. Their support was crucial in my completion of the program.

THIS PAGE INTENTIONALLY LEFT BLANK

CHAPTER 1:
Introduction

The demand for energy continues to grow as the U.S. military must address conflicts across the globe and assist with humanitarian assistance missions. Operational sustainability requires optimal energy use, especially in rugged and extreme environmental conditions. The increasing energy cost is a burden on the defense budget, taking away resources that could be invested in improving our military capabilities. Additionally, uncertainty associated with environmental conditions influences the design of an effective expeditionary power grid. The allocation of limited military resources to establish forward operating bases (FOBs) requires careful analysis of energy needs and resources.

This thesis builds on the mathematical optimization model in [1] which exploits physical characteristics of heating ventilation and air conditioning (HVAC) systems and the energy sources that power them. Our study evaluates uncertain factors contributing to temperature differences in an expeditionary environment, using a design of experiment (DOE) approach to gain insight into the performance of the optimization model under a variety of circumstances. Some of the findings may also support the development of a robust version of the optimization model.

1.1 Department of Defense and Energy

The world's largest energy consumer, the Department of Defense (DOD), uses more energy in daily operations than any other private or public organization [2]. Comprising is not the right word here. The DOD consumes more energy than all other federal government agencies combined, which amounts to approximately 80% of the total U.S. government consumption [3]. The DOD's energy use falls into two distinct categories: operational and installation or facility energy. In fiscal year (FY) 2014, operational energy accounted for 70% of the department's energy usage; DOD used over 87 million barrels of fuel, at a cost of nearly $14 billion [4]. Figure 1.1 shows the DOD's energy consumption over time. In 2008, the DOD accounted for 0.8% of the nation's energy consumption, which is the equivalent of burning 395,000 barrels of oil per day. To put that figure into perspective, the DOD consumed about as much energy as needed to power the entire country of Greece [2].

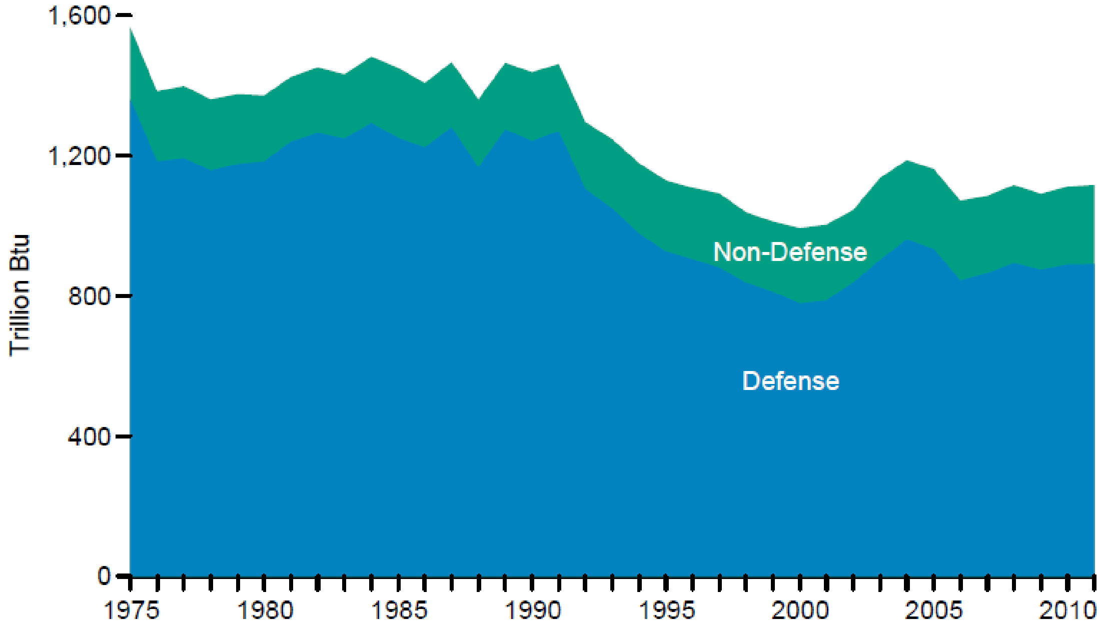

Figure 1.1. U.S. Government Energy Consumption by Agency (Defense vs. Non-Defense), Source [5].

To ensure the uninterrupted flow of electrical energy for military missions, most of the expeditionary and other DOD FOBs rely on fossil fuel-based generators to power equipment and systems for military operations. Although renewable energy currently flows into the power grid, fossil fuel-based energy far outstrips all other sources for DOD operational energy. Over a decade of war in Afghanistan and Iraq has drawn greater attention to the need for effective management and use of operational energy. To limit fuel usage, the DOD is identifying ways to reduce consumption. Figure 1.2 depicts the breakdown of U.S. operational energy consumption for FY 2014 by domain, service, mission, and combatant command.

Each service spends a substantial amount of its budget on electrical power generation for operations across the globe. Air operations represent most of DOD's operational energy usage. The U.S. Central Command (CENTCOM) is also a major consumer of energy, given the Iraq and Afghanistan wars. Air Force operations represent more than half of the entire DOD operational energy requirements [6]. The Navy's operational energy requirements come from air operations as well as ships sailing around the world to maintain the freedom of commerce at sea. In years past, the Army and the Marine Corps accounted for the

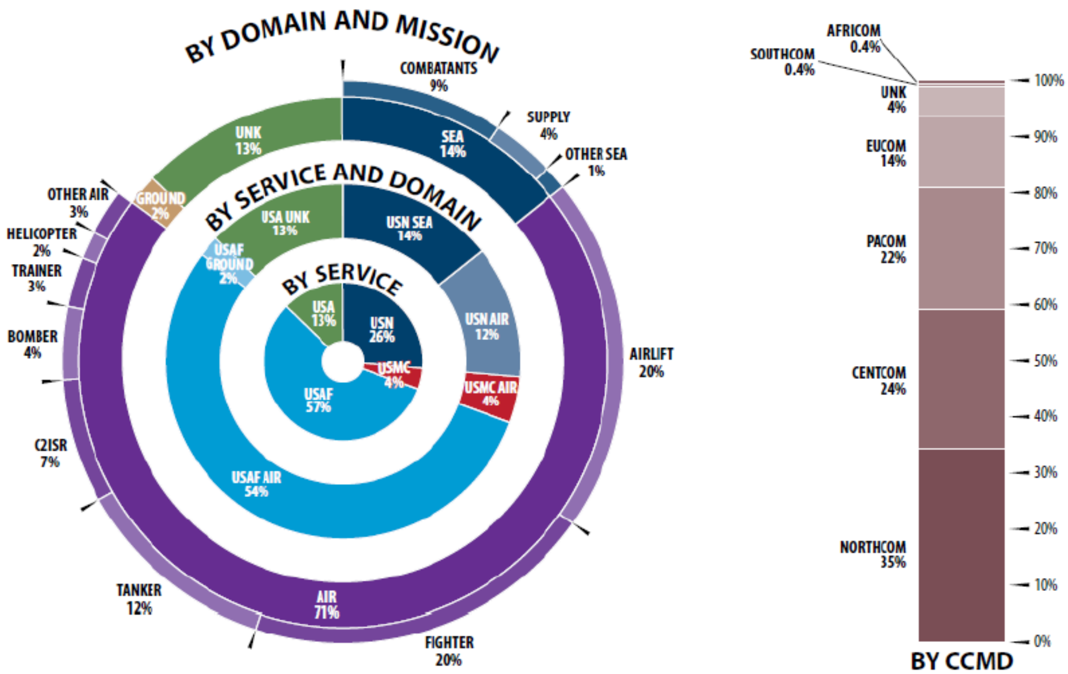

Figure 1.2. Operational Energy Use, FY 2014, Source [6].

lowest consumption annually among the branches of service; however, this changed after the two recent wars when fuel requirements to support electricity generation and fuel costs skyrocketed. In FY 2013, the department used more than 9 million barrels of liquid fuel to support Operation Enduring Freedom in Afghanistan [7]. Table 1.1 shows that as the operational tempo increases, the demand for fuel also increases.

Category	Peacetime OPTEMPO	Wartime OPTEMPO
Combat Vehicles	30	162
Combat Aircraft	140	307
Tactical Vehicles	44	173
Generators	26	357
Non-Tactical	51	51
Total	**291**	**1040**

Table 1.1. Army Fuel Consumption in Peacetime and Wartime (Million Gallons per Year), Source [8].

Table 1.2 displays some interesting observations of researchers in the Expeditionary Energy Assessment Environmental Control Unit Alternatives Study conducted for the Marine Corps Expeditionary Energy Office. The Marine Air-Ground Task Force (MAGTF) Power and Energy Model, (MPEM) uses data from Afghanistan and the operational cost of fuel at $6.39 per gallon to calculate savings in dollars. The result demonstrates that a 10% increase in efficiency from the current environmental control unit (ECU) suite requires only a nominal investment and the gain is technically feasible [9]. The subsequent increase in efficiency produces substantial savings that cannot be ignored. However, such savings naturally depend on the unit's mission and the theater of operation. The 2009 field data from the USMC Afghanistan study concluded that generators averaged a load of 30%; additionally, the HVAC represents 75% of the electrical demand and wastes 50% on inefficient structure [9]. Optimizing the HVAC control system and improving the efficiency of living structures is one of the most effective ways to reduce energy consumption. We analyze a model optimizing HVAC control systems in this research.

	Annual Fuel Savings in Tankers and Dollars			
	10% ECUs	20% ECUs	30% ECUs	Solar ECUs
Tankers of Fuel	79	158	217	487
Savings (Millions)	$2.42	$4.85	$6.65	$14.95

Table 1.2. Annual Fuel Savings in Tankers and Dollars, Source [9].

1.2 Cost of Environmental Temperature Control

In military operations, the cost of environmental control sometimes exceeds the cost associated with the equipment used in the mission. Overall costs include the energy used to power the equipment as well as to sustain it. The sustainment costs in combat and hostile environments sometimes outweigh everything else when there are human lives involved. In Leslie Hayward's interview with the first-ever Assistant Secretary of Defense for Operational Energy Plans and Programs, Sharon Burke, she stressed that the DOD is ultimately a business, and that energy is a variable cost that must be kept down [10]. However, unlike

business, the DOD often engages in warfighting in which energy is both a liability and an opportunity [10]. We treat this energy cost as a liability in terms of fuel consumption, and review the impact of environmental temperature conditions on fuel consumption in fulfilling military missions.

1.2.1 Monetary Costs

Among numerous other reasons, the volatility of the world oil market makes it highly desirable to reduce the demand for operational energy. In 2010, the DOD consumed nearly 5 billion gallons of petroleum in military operations, costing $13.2 billion, a 255% increase over 1997 oil prices [11]. The volatile price makes it difficult to accurately estimate and budget for fuel costs [11]. Overall, every $10 increase in the price of a barrel of oil increases the price of DOD operations by $1.3 billion [2]. To put this value in context, each $10 price increase is equivalent to the loss of almost the entire procurement budget of the U.S. Marine Corps (USMC) [2]. These estimates also do not account for the cost of transporting fuel to desired locations, which varies depending on the modes of delivery and the situation on the ground. For example, an Office of Naval Research (ONR) report found that the fully accounted costs (including transportation, storage, and logistics expenses) for a gallon of gasoline on the battlefield in Iraq and Afghanistan actually ranged from $15 per gallon to as much as $400 per gallon [2]. In-flight delivery of fuel for the Air Force costs approximately $42 per gallon [2].

Additionally, electricity generation constitutes a significant portion of operational energy usage on the battlefield. A late 2009 study conducted by the Marine Energy Assessment Team (MEAT) in Afghanistan revealed almost 89,000 gallons of daily fuel usage; out of this, power generation accounted for about 32% of the consumption [12]. HVAC systems alone used approximately 75% of the power generated [12]. To put this amount into perspective, of about 28,500 gallons of daily usage, HVAC systems consumed 21,000 gallons, costing about $22 million annually at $2.80 per gallon for the Marine Expeditionary Teams at the FOB used in this study. Also, the study uncovered the drastic growth in cost per gallon on the battlefield when approaching the tactical edge. This makes our $2.80 per gallon quite an optimistic estimate. The cost growth reflects the logistics involved in delivery. Figure 1.3 displays this cost growth.

Figure 1.3. Cost Growth Approaching The Tactical Edge, Source [12].

This cost burden deprives the DOD of funds that could be invested in other programs to enhance capabilities to deal with new threats to national security.

1.2.2 Other Costs

The cost growth, when approaching the tactical edge also comes with a human cost. The most frequently employed tactic during warfare is deny or disrupt resupply to the opposing forces. The weapon of choice commonly used on coalition forces' fuel convoys in Iraq and Afghanistan has been improvised explosive devices (IEDs). This choice makes human life another variable, depending on the level of sophistication of the opposing forces, the terrain, and the weather of the battle space. DOD officials reported that in June 2008 alone, a combination of these factors resulted in the loss of about 44 trucks and 220,000 gallons of fuel [13]. Figure 1.4 illustrates the human cost of fuel resupply in Iraq.

This figure shows that, between July 2003 and May 2009, IEDs accounted for about 43% of U.S. fatalities, a reminder of the fuel resupply burden in warfare operations. The manpower and equipment requirements to protect the logistics route represent another cost factor. Minimizing the fuel requirements will free up these resources for other missions.

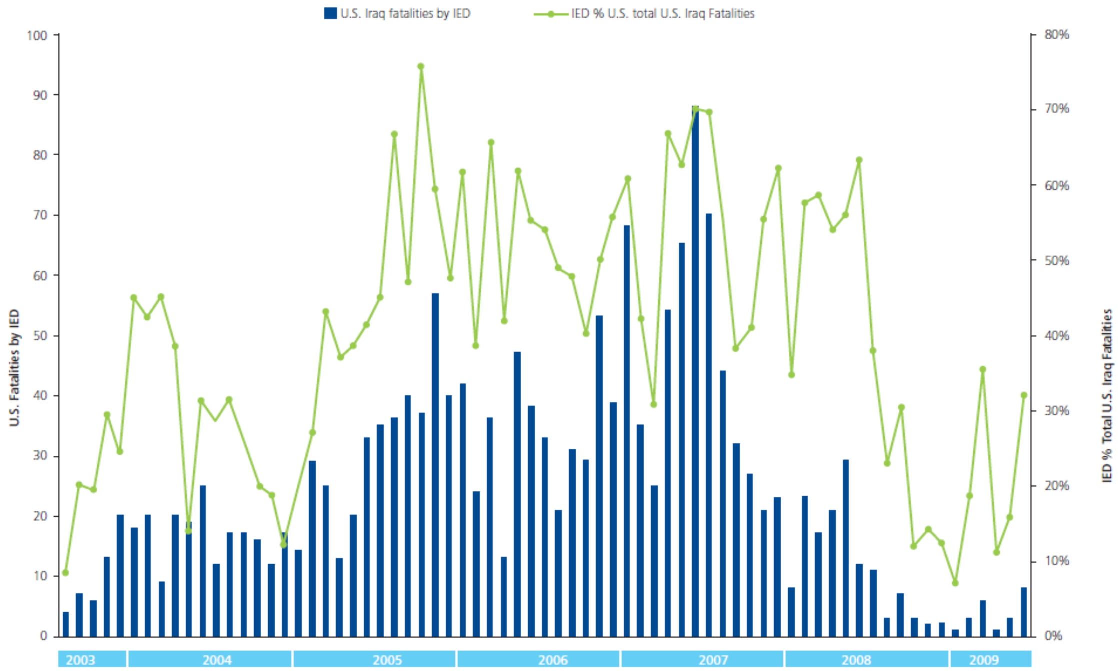

Figure 1.4. U.S. Fatalities in Iraq by IED, Source [13].

1.3 Energy Technology Initiatives and Opportunities

The DOD recognizes this opportunity for savings and is investing substantial resources in energy initiatives. As part of the FY2013 budget, the DOD requested more than $1.4 billion for operational energy initiatives [3]. The DOD's five year (FY2013–FY2017) Future Year Defense Plan (FYDP) includes a total of about $8.6 billion for operational energy initiatives [3]. The aim is to reduce the demand for energy required to conduct operations around the world. Table 1.3 shows some of these DOD energy initiatives.

The rapid fielding of equipment in theater is one initiative designed to streamline the deployment of equipment, such as more efficient generators, to reduce in-theater fuel consumption. The implementation comes with the challenge of generator load and efficiency management.

Cyclical loads from operating HVAC systems at FOBs present a unique obstacle to achieving maximum efficiency of the installed energy system. Environmental conditions, equipment operations, and mission requirements often determine the load requirements that should be planned for when setting up the FOBs. As the load requirements vary throughout the

Initiative	Description
Establish a baseline of DOD operational energy consumption	Gather reliable DOD-wide data on operational energy consumption, to serve as a foundation for analyzing DOD operational energy use and developing operational energy metrics.
Defense Operational Energy Board	This board oversees the execution of the Operational Energy Implementation Plan, including setting operational energy metrics.
Rapid fielding of equipment in theatre	Efforts to streamline the deployment of equipment (such as more-efficient generators) that reduces in-theatre fuel consumption,
Operational Energy Capability Improvement Fund	$19.5 million fund to spur technology innovations that reduce energy load at contingency bases, measure energy consumption in forward areas, and transform waste into energy.
Energy Key Performance Parameter	Establish a methodology for an Energy Key Performance Parameter (KPP) to be used in requirements gap analysis, requirements development, and acquisition programs.
Fully burdened Cost of Fuel	Provide the services with non-binding guidance on the methodology and application of Fully Burdened Cost of Energy (FBCE) estimates as part of the life-cycle cost analysis for new capabilities during the acquisitions process.
Energy in Procurement Contracts	Work with DOD's office of Defense Procurement and Acquisition Policy to develop template language on energy performance for DOD contracts.

Table 1.3. Major ASD (OEPP) Operational Energy Initiatives, Source [3].

day, effective administration of the unmanaged requirements plays an important role in the efficiency realized from the installed capacity. Improving the efficiency of the installed capacity is critical to minimizing the generators' fuel consumption.

1.3.1 Load Sizing Peak and Average

Sprague describes a four-step process that expeditionary energy systems use when analyzing the load requirement for a typical FOB [1]:

1. Determine the type, quantity, and characteristics of connected loads in each structure or facility [1].
2. Calculate the theoretical maximum power requirement of a facility if all connected equipment is simultaneously operating [1].
3. Adjust this maximum value by applying a demand factor (≤ 1) representing an assessment of the realistic portion of facility equipment that would simultaneously operate [1].
4. Add allowances for future growth [1].

The current system requires the demand for air conditioning to be weighted by a demand factor of 1.0 [1], requiring the energy system to meet the full power requirement at all times. Unfortunately, environmental weather conditions can be very unpredictable, often leaving the generator with excess capacity. This excess capacity can lead to inefficient expeditionary energy systems.

Sprague's generator output simulation revealed that, when connected loads operate at a 75% duty cycle, the average power demand is 21.6 kilowatt (kW) and the peak demand is 28.8 kW, resulting in high generator usage. On the other hand, at a 25% duty cycle, the result is the opposite with substantial wasted capacity and the generator frequently running below a 30% load, leading to more fuel burned inefficiently [1]. Field data from Afghanistan in Figure 1.5 displays the historical generator load from electrical demand.

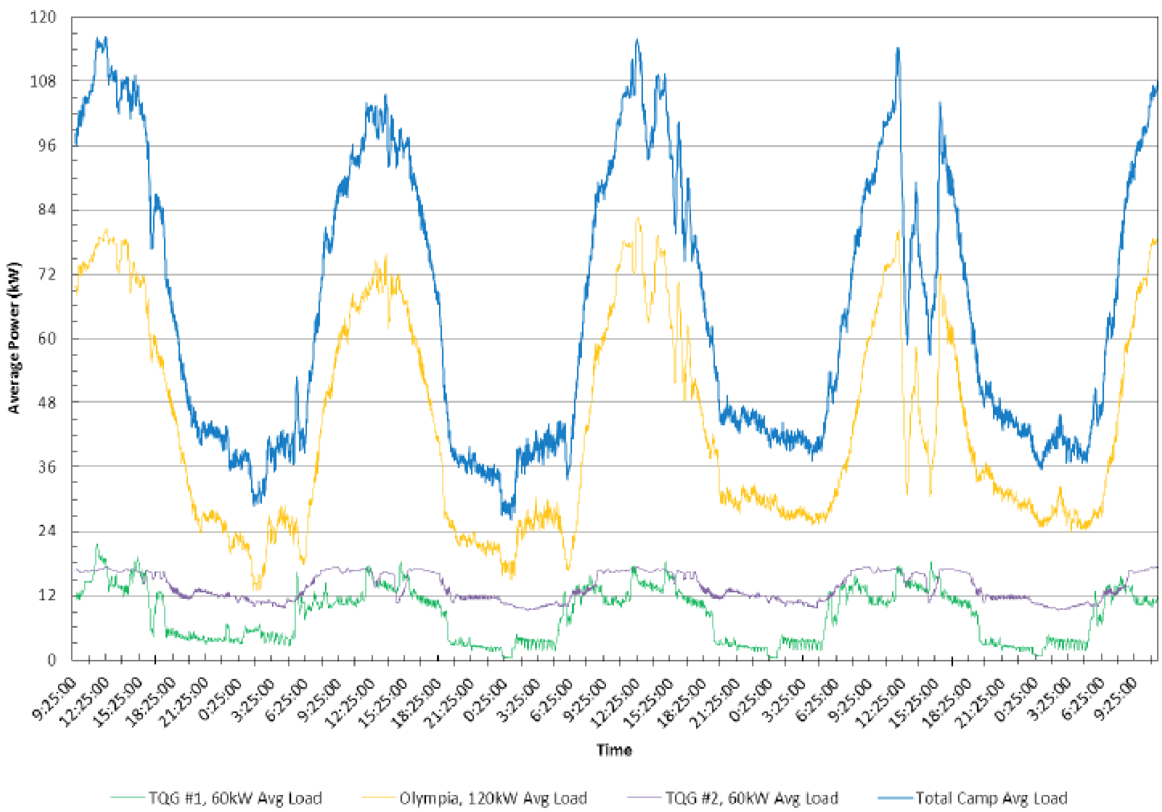

Figure 1.5. U.S. Forces Afghanistan Camp Electrical Demand Over a 96-Hour Period, Source [1].

1.3.2 Generator Fuel Efficiency

Fossil fuel generators convert the chemical energy of the fossil fuel into the electrical energy used to power expeditionary energy systems. The generator efficiency is the ratio between the useful electricity outputs in a specific time unit to the chemical energy supplied from the fuel within that same time. Often, this efficiency is less than 50% with most efficiency lost to heat generated during the conversion process. However, with an accurate estimation of the load factor, larger Tactical Quiet Generators (TQGs) tend to be more efficient than smaller units. Figure 1.6 illustrates the relationship between load factor and fuel efficiency by TQGs sizes [1].

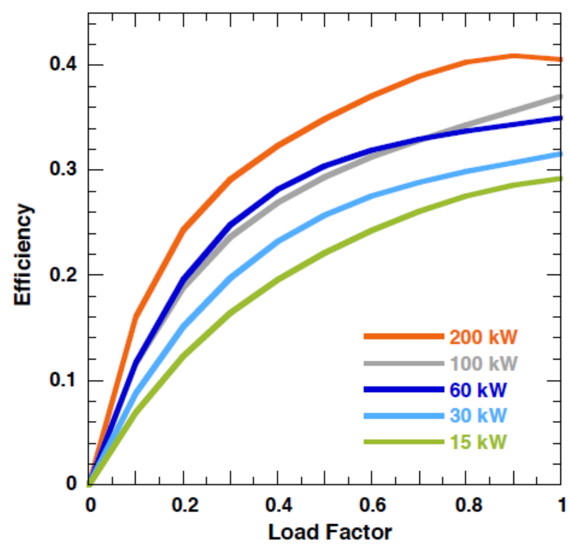

Figure 1.6. U.S. Military TQGs Fuel Efficiency as a Function of Load Factor and Generator Size, Source [1].

Selecting the smallest generator capable of providing the required power achieves maximum efficiency [1]. Sizing generators with load requirements based on the peak power demand, rather than the average power demand, creates inefficiency during low- and average-demand periods, which happens regularly.

1.4 Research Objectives

This research study investigates the impact of uncertain factors influencing fuel consumption in an expeditionary power grid. We conduct a multifactor-designed experiment of key input

parameters in Sprague's optimization model to tease apart specific contributions to fuel savings. We vary the uncertain factors to understand specific effects on the cumulative total fuel consumption, as well as to obtain useful insights into generator behaviors in the model. Our analysis of the impact of uncertainty on Sprague's optimization model may also support the future development of a robust version of the optimization model.

1.4.1 Scope

This research employs the principle of DOE using the nearly orthogonal Latin hypercube (NOLH) design to vary uncertain input parameters in Sprague's model. We extend the research beyond Sprague's baseline power grid set-up by changing the energy production configuration, and introducing patterns for renewable energy production and unscheduled demand. This allows us to analyze how well Sprague's model handles varying, uncertain environmental conditions, as well as assess the results of operating under these conditions.

1.4.2 Thesis Contribution and Outline

This thesis complements industry and government progress in the field of efficient tactical hybrid power systems and reduced energy demand. The analysis of optimized load scheduling provides more insight into practical considerations for using this optimized load scheduling approach.

Chapter 2 presents a literature review of the academic, commercial, and government studies that inform our present research. In Chapter 3, we describe the model developed by Sprague, and our DOE methodology that investigates uncertain factors influencing generator fuel consumption. Chapter 4 presents our findings, and Chapter 5 contains the conclusion and future work.

THIS PAGE INTENTIONALLY LEFT BLANK

CHAPTER 2:
Literature Review

Both the government and industry often discuss the optimization of electric power generation from various energy sources. The U.S. military, in particular, has invested heavily in initiatives and research to improve efficiency on generators, ECUs, and structures used at FOBs for conducting military operations. In his thesis, Sprague highlights the intersection of three fields of research and application: military energy efficiencies, hybrid smart microgrids, and demand side management [1]. In contrast, this thesis draws from the previous work and evaluates uncertain factors contributing to temperature differences in an expeditionary environment, using a DOE approach to gain insight into the performance of the optimization model under a variety of circumstances. Some of the findings may also support the future development of a robust version of the model analyzed.

We review a brief description of the expeditionary energy power system, energy efficiency trade-offs and power generation, distribution systems, and the principles of the design of experiments.

2.1 Expeditionary Energy Power System

A tactical expeditionary energy power system will consist of some combination of a power generation subsystem, a distribution subsystem, and the electrical loads requirements of the customers. Also, energy storage is sometimes incorporated into the power system to enhance its resilience and efficiency. Figure 2.1 depicts a general representation of a typical expeditionary power system. Sprague provides a more detailed description of the expeditionary system and various energy system architectures [1].

2.2 Energy Efficiency Trade-offs and Power Generation

Recent developments include the following: more efficient power generators; better insulated structures; intelligent, software driven controllers for distribution; and more efficient demand side equipment drawing power from the grid. Energy efficiency trade-offs abound in electric load management. Electric load management is a specific way of controlling

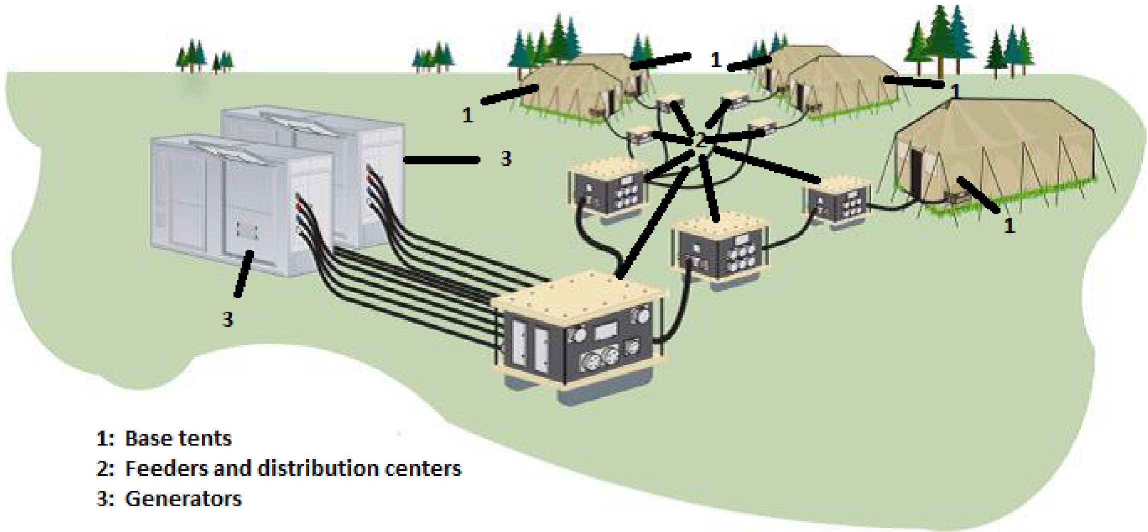

Figure 2.1. Expeditionary Energy Power System Set-Up, Adapted from [14].

the peak load in the network to produce a constant or average demand [15]. This process involves both the supply-side and demand-side management of power requirements.

Efforts to reduce generator fuel usage and cost have motivated some academic research in recent years. A Naval Postgraduate School (NPS) student, R. Kelly [16] investigated the benefit of transitioning from traditional generator employment to an alternative architecture using an Energy Management System (EMS). The EMS provides an intelligent interface by matching real-time load demand to the smallest capable power source to reduce fuel consumption between various power sources, loads, and energy storage elements to form a microgrid [16]. T. Mansfield et al. [17] at the United States Military Academy created a prototype Hybrid Tactical Power System (HTPS) by drawing energy from various sources to address the low-peak load variability problem via load aggregation for a more efficient use of generators, therefore reducing fuel usage and generator maintenance cost. Bouaicha [18], a student at NPS, examined a Hybrid Electric Grid (HEG) model that uses weather forecasts to establish an optimal day-ahead schedule for the grid in a robust and cost efficient manner. Another NPS student, Ulmer [19], extended this research further with a capital planning optimization model by using historical solar data and simulated forecasts for wind data to formulate a mixed integer linear program that maximizes the islanding time of a microgrid, subject to budget and physical constraints. Islanding time is the amount of time demand can be met without a connection to the commercial power grid.

The commercial utility industry, the supply side, studied the demand pattern from consumers, the demand side, for over a decade to establish a pricing system that would influence power demand requirements. Unmanaged peak load power demand requirements will eventually require utility company to increase generation capacity to meet the increasing demand. Increased capacity becomes excess during the minimum and average load periods, therefore creating an inefficient and expensive energy system. To reduce the peak load period and bring it closer to the average load period, the pricing mechanism incorporates an incentive pricing system. It requires the shiftable cyclic load to be delayed until the beginning of the minimum or average load demand period for better pricing. The design allows either the customers or the utility company to control load shifting during the peak period [15]. Figure 2.2 displays what the utility company aims to achieve with this approach. The end result is the demand side with a lower bill and the supply side with a reduced peak load, increased load factor, and improved efficiency [15].

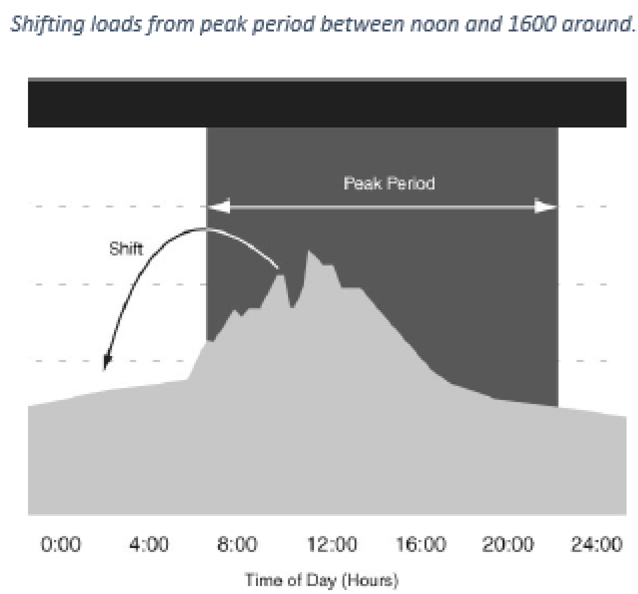

Figure 2.2. Peak Load Shifting, Source [15] .

On another note, efficiency trade-offs in the military have been mostly pursued with the introduction of more efficient generators and the addition of hybrid power plants [1]. From TQGs to Advanced Medium Mobile Power Sources (AMMPS) and Ground Renewable Expeditionary Energy Network Systems (GREENS), improving efficiency continues to dominate the DOD's effort at reducing the energy demand at FOBs. The recent effort of the

U.S. Army "The Tactical and Deployed Power" includes the 1 kW multi-fuel generator, an alternative energy hybrid generator that provides intelligent, tactical, and convenient squad level power [20].

2.2.1 Renewable Energy Power Generation

Renewable energy sources provide the expeditionary power generation system the resilience required to sustain longer operations without relying too much on fossil fuel energy. Although still being continuously researched, solar-powered unmanned aerial vehicles (UAVs) will provide the DOD a great option to reduce fuel consumption in expeditionary units. The top companies currently using this technology and their popular solar UAVs include the following:

- The Airbus – Zephyr
- Boeing Phantom Works – SolarEagle
- Google Titan Aerospace – Solara
- Facebook Ascenta – High-speed internet via drones
- AeroVironment/NASA – Gossamer Penguin, Solar Challenger, NASA Pathfinder (Plus), NASA Centurion, NASA Helios
- Lockheed Martin – Hale-D

The Renewable Energy for Distributed Under-Supplied Command Environment (REDUCE) [20] is a program developed by the U.S. Army Communications Electronics Research, Development and Engineering Center. It is a state-of-the-art system enabling the harvesting and use of solar and wind power, energy storage, energy distribution and monitoring, and mobility; it can produce up to 5 kW of power in the field. As shown in Figure 2.3, it can be moved around easily with its light tactical flat deck trailer mount, making it easy to be placed in a position of maximum utility and performance.

Solar-powered ECU, produced by SunDanzer, an El Paso-based commercial firm in business since 1999, employs solar panels to power a cooling only ECU when there is sufficient sunlight, without using batteries for storing excess power for future usage [9]. Figure 2.4 shows a typical set-up for this system. The direct current air cooler (DCAC) model developed by National Aeronautics and Space Administration (NASA) and licensed to SunDanzer uses

Figure 2.3. REDUCE, Source [20].

a patented refrigeration technology in its design by optimizing the refrigeration cycle to achieve low energy consumption [21].

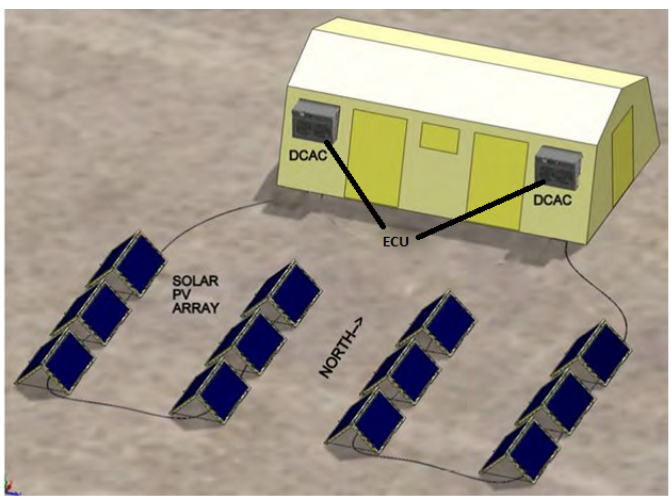

Figure 2.4. Solar Powered ECU, Adapted from [9].

2.2.2 Other Power Generation

The traditional approach to power generation uses fossil fuel-powered generators. The Project Manager for Mobile Electric Power (PM MEP) is the DOD executive agent that oversees the battlefield electric power generation and integration. Figure 2.5 shows the organizational chart. PM MEP missions are as follows [22]:

- Establish, maintain, and standardize a DOD-wide family of Mobile Electric Power Generating Sources (MEPGS), including the development of the best mobile generators.
- Execute program, including consultation on how to improve and expand standardization MEPGS across the DOD.
- Approve and disapprove all requests for non-standard MEPGS.

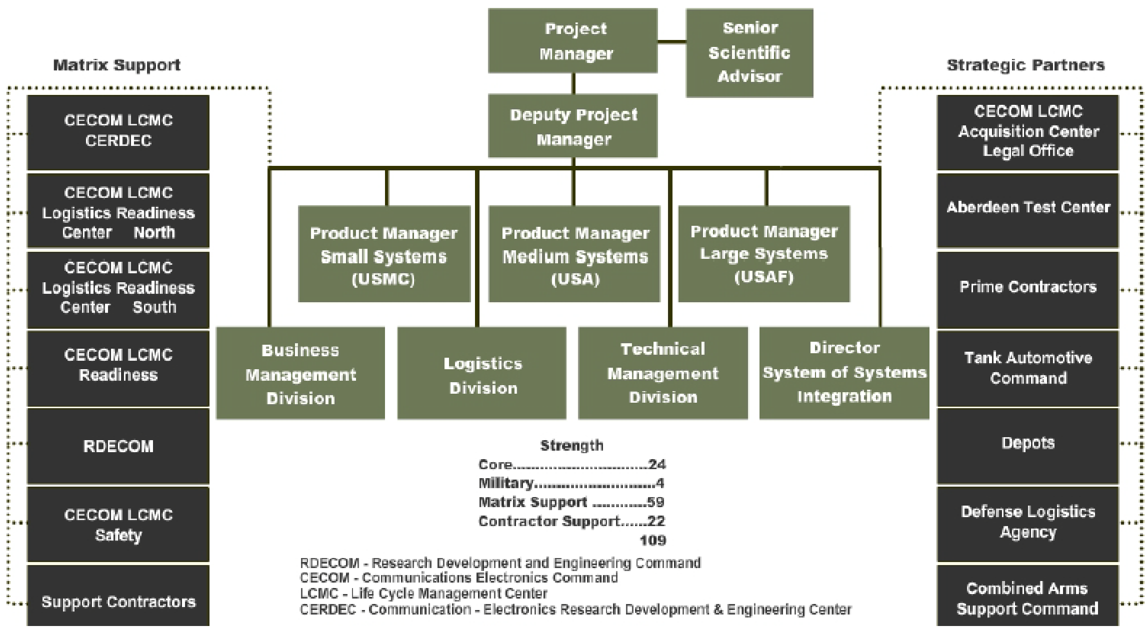

Figure 2.5. Team MEP Organization Chart, Source [22].

The PM MEP assisted in the DOD transition from the TQGs to AMMPS as one of the measures to improve efficiency in power generation. The Office of Naval Research (ONR) is spearheading collaboration with academia, industry, and the PM MEP on the use of modular, compact solid oxide fuel cell (SOFC) generators for tactical electrical power, which will provide highly efficient silent power generation that is towable for mobile tactical units.

2.2.3 Energy Storage and Power

With an energy storage device built into the system, the power grid's resilience can be improved. Recent advances in technology have improved the storage capacity and length of time for battery energy storage. The DOD collaborates with industry, government agencies,

and academia to improve energy storage for operational use. The Hybrid Energy Storage Module (HESM), shown in Figure 2.6, is a collaborative effort between the DOD and the Department of Energy to develop a scalable storage platform for military and commercial use [23]. More information on energy storage can be obtained from Sprague [1].

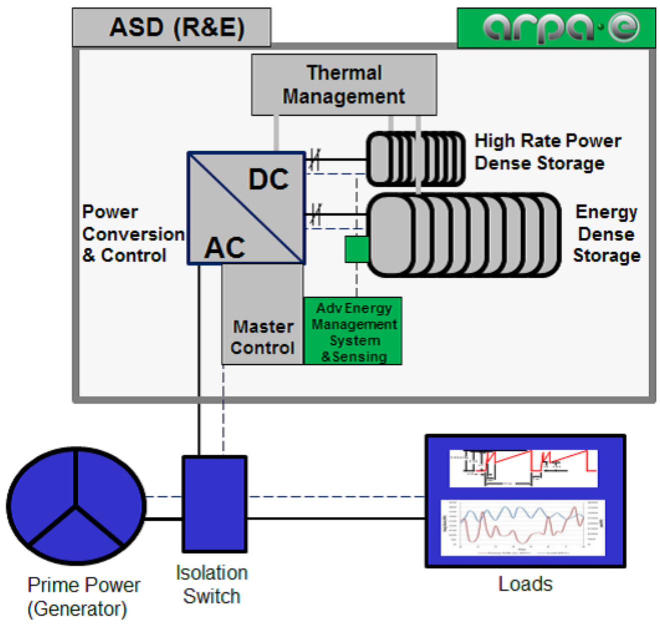

Figure 2.6. Energy Storage Module, Source [23].

2.3 Distribution Systems

The DOD conducts operations mostly away from existing installations where infrastructures already exists. The operation site's energy requirements must be generated on-site, through an efficient power generation system, and distributed through an intelligent system. Figure 2.7 illustrates such a distribution system. Previous design efforts focused on how to supply and distribute power whenever required at the right quantity. Today's distribution efforts address properly sizing and distributing energy to obtain an efficient energy system. It involves the design of an intelligent microgrid system that is capable of addressing the following:

- Development of real time and non-real time models, simulation, and optimization to support designs that are adaptable to multiple components, devices, and systems on the grid [23].

- Robust and flexible bi-directional power control at power densities suitable for multiple platforms [23].
- Integrated hardware, open architecture design and intelligent automatic control, and a unified management system.
- Power converters and inverters enabling interoperability.

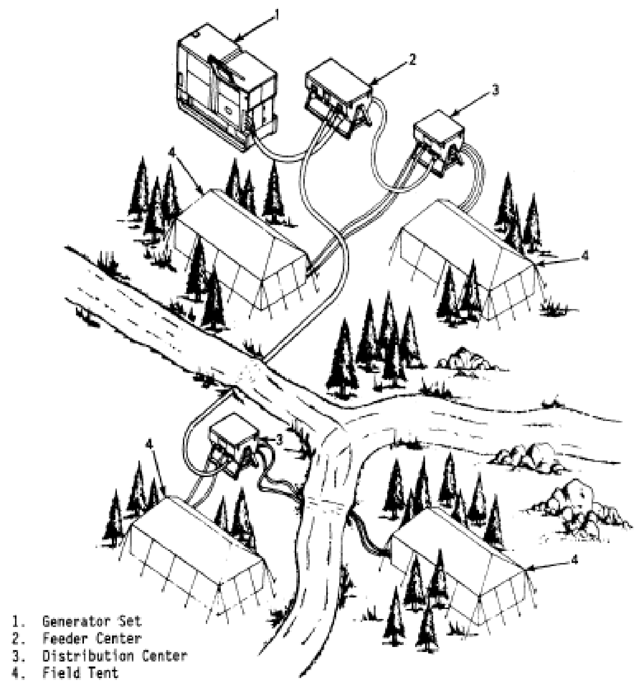

Figure 2.7. Typical Distribution System, Source [24].

The opportunity for an intelligent power management system can be pursued through networking, advanced sensors, and control software and hardware. The future of the current Power Distribution Illumination System Electrical (PDISE) is intelligent power distribution, in which every component in the system is driven by model software that can sense and predict requirements on a continuous basis, and then distribute loads in the most efficient and optimal manner. Figure 2.8 displays the ultimate goal. This thesis contributes toward this field of research. Our analysis of the impact of uncertainty on the optimal scheduling of an electrical load model will shed more light on the areas that require more attention.

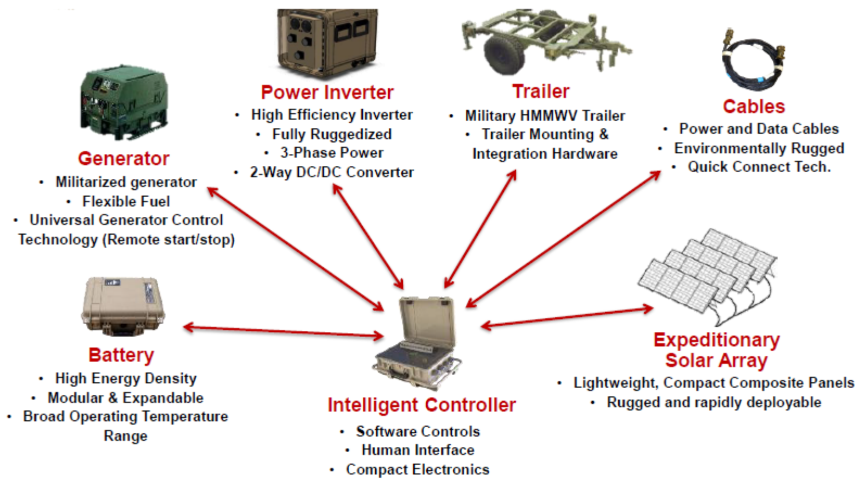

Figure 2.8. Intelligent Power Distribution System, Source [14].

2.4 Design of Experiments

Every day the world, including systems and processes around us, continues to become more complex. Making any informed decision on designing future systems and processes requires understanding today's complexities and the factors contributing to this complex behavior. Design of experiments (DOE) is a powerful tool that enables researchers to gain insight into cause-and-effect relationships that characterize our complex world. Central to the principle of DOE are models or systems with input parameters or factors, undergoing a process or transformation to produce one or more outcomes. Each outcome is called a response whose behavior depends, in part, on the input factors called the predictors. Scholars continue to investigate and research options for generating designs that allow analysts to gain insight efficiently and effectively when running experiments.

DOE dates back to the work of Fisher [25], a mathematician whose pioneering effort mostly dealt with applications in agriculture. Some of his discoveries include the analysis of variance (ANOVA), principles of blocking and randomization, and Latin square and split plot experiments [26]. Many designs intended for physical experiments focus, by necessity, on varying only a few factors and severely limiting the number of design points. More recently, large-scale designs suitable for large numbers of factors have proven to be very beneficial for simulation experiments; examples and references are provided in [27]

and [28]. For example, Sanchez et al. [27] highlight the importance of using large-scale designed experiments in defense and homeland security applications. Their simulation experiment involving a hybrid optimization model for unmanned aerial vehicle surveillance demonstrates this significance, saving an estimated $20 billion for the U.S. Army [27]. Space-filling designs like the Latin hypercube, the orthogonal Latin hypercube, and the NOLH are useful .

Application areas of DOE are expansive and continue to grow. As just one example, over 160 theses and numerous papers involving simulation experiments appear on the web pages of the NPS's SEED (Simulation Experiments & Efficient Designs) Center for Data Farming [29]. Those most closely related to this work evaluate optimization models. For example, Gardner [30] conducts a series of experiments on a two-stage stochastic optimization model for planning naval logistics functions in humanitarian assistance operations, and Li [31] uses a similar approach to find a model for planning the military response following typhoons in Taiwan. Gardner and Li both find that the results of changing the inputs to the optimization model in a designed experiment yields useful insights about its performance and robustness. Morse [32] investigates the robustness of an optimization model to predict future energy needs and costs for Marine Corps expeditionary operations, including the use of solar energy; the robustness of his results in the presence of correlated cost coefficients is further explored in Sanchez et al. [33].

CHAPTER 3:
Methodology

Sprague's "Optimal Scheduling of Time-Shiftable Electric Loads in Expeditionary Power Grids" model minimizes fuel consumption by prescribing an optimal schedule for generator operation, ECU utilization, and energy storage management in a deterministic manner. The model considers the physical constraints of generator and ECU operation, as well as thermal constraints that must be satisfied within the internal structures in expeditionary FOBs [1].

We first provide a brief description of Sprague's model. We then lay out two designed experiments that assess the performance and robustness of this model under varying conditions.

3.1 Sprague's Optimization Model

A detailed description of Sprague's model can be found in Chapter 4 of his thesis, but we summarize its features to better explain our contribution to the research.

Sprague's model makes a set of assumptions for simplification; the thermal model is the principle constraint that must be observed to maintain the structure's internal temperature within acceptable limits; and the formulation of the optimization model, which incorporates the assumptions and thermal model.

3.1.1 Objective

Sprague's optimization model is a discrete-time mixed integer linear formulation that minimizes generator fuel consumption. It uses prescriptive mechanisms for periods of ECU operation, subject to specific internal structure temperature requirements, and the physical limitations of equipment.

The objective is to minimize total fuel consumption, subject to a number of constraints. The complete list of constraints with their general descriptions can be obtained from Sprague [1]. Some of the constraints include those for keeping the temperature within a specific range, those that ensure power requirements properly match power production, those that

limit generators' start and stop times, and so on. Sprague studies several variants of the optimization algorithm, but we focus on two that seemed to perform well and reflect real-life application: rolling horizon with perfect future knowledge (RH-PFK) and rolling horizon with uncertainty (RH-U). Both models are run in a rolling horizon fashion, meaning that they iterate over time steps by optimizing over a planning horizon and then executing that plan over a shorter execution horizon. Following execution, the models then advance their planning horizon forward by the length of the execution horizon, repeating this process until all time steps have been considered [1]. The RH-PFK receives perfect knowledge during this process, meaning that the parameter values it encounters during the planning process are the same as it encounters during the execution process. The RH-U, on the other hand, receives a set of constant forecasted values for planning purposes and the actual values during execution. For demonstration purposes, Sprague generates actual demands from a specified uniform random distribution with constant expected value [1]. For our experiments, both models receive the same sets of actual parameter values. We describe our process for generating these values in Sections 3.3 and 3.4.

3.1.2 Model Assumptions

The following assumptions ensure model simplification and computational tractability and help to bridge the gap from shortfalls in data availability and computation power:

- Loads are balanced in each period and commensurate with the total load of all operating generators split among them according to their nameplate rated capacity [1].
- The charge and discharge rate limits of energy storage devices are constant for the range of the battery level, and the level varies linearly with the chosen charge and discharge rates [1].
- All power production is aggregated and available to any load within each period [1].
- Software tools not independently validated with field or test data provide estimates of the thermal behavior of shelter and ECU performance [1].
- Generator fuel consumption is modeled as a piecewise linear curve of rated power [1].

3.1.3 Thermal Model

At any point in time, the internal structure temperature is a function of the external environmental temperature or conditions, the physical structure characteristics, and the ECU work

output [1]. Although the model is similar regardless of whether heating or cooling is being considered, Sprague only considers cooling for the sake of simplicity [1], and we will do the same.

3.1.4 Inclusion of Variability

Sprague accounts for uncertainty variability with the introduction of three parameters: unmanaged demand, renewable production, and the heat transfer intercept. Both variants are run using the same sets of actual values, randomly generated from Uniform distributions centered around the expected values, with floors of zero to prevent negative results [1]. Sprague's model parameters use the following uncertain data as inputs.

- Unmanaged or unscheduled demand consists of demand from the customers that arises from the unplanned use of equipment such as ironing clothes, using the microwave to prepare meals, charging electronic devices, and so on.
- Renewable production comes from sources that include solar, wind, hydroelectricity, and so on. Power production from these sources varies throughout the course of the day.
- The heat transfer intercept represents the shelter equilibrium heat transfer rate, which determines how fast heat affects the shelter. The environment adds heat to the shelter, as do the equipment and personnel within the shelter. The intercept parameters depend on the characteristics and type of shelter. For instance, wooden and brick shelters will have different mean heat transfer intercepts. The intercept may vary during the course of the day as a result of people entering and leaving the shelter.

3.2 Baseline Scenario

Sprague uses data from Afghanistan to derive his model parameters [1]. We use many of the same values; our baseline scenario also uses a time step of two minutes, and assesses the performance over 300 time steps (a ten-hour day). This baseline sets up our first designed experiment in this research.

3.2.1 Model Baseline Composition

The baseline grid configuration models a U.S. Marine Corps (USMC) patrol base in Afghanistan with 45 Marines, sheltered in eight structures, using 10 ECUs, three conventional generators, and three hybridized generators with battery storage [1]. Figure 3.1 provides a general overview of such a power grid.

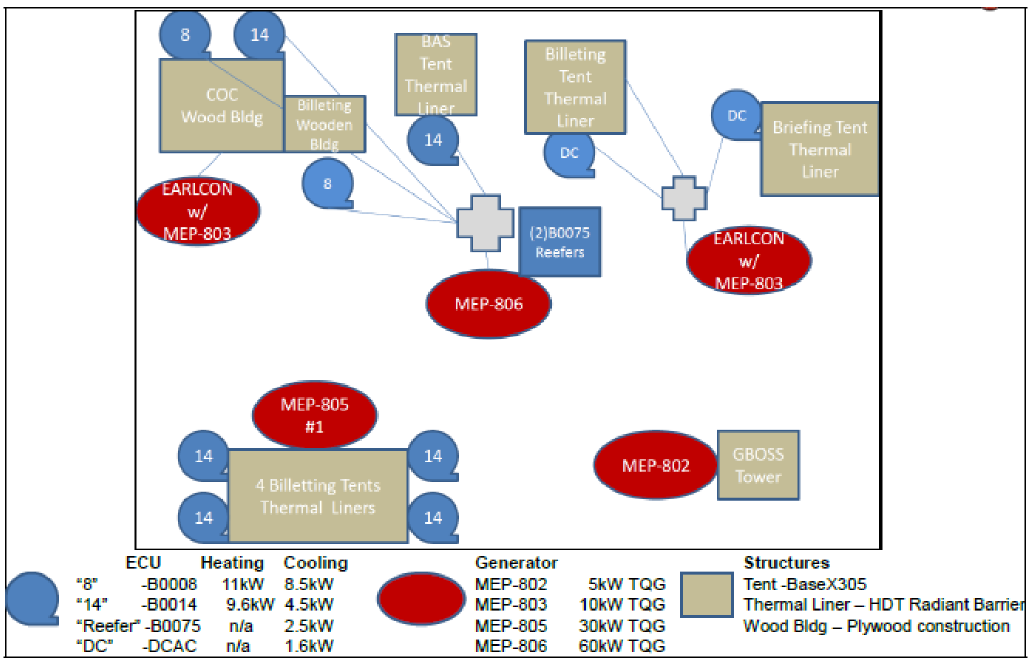

Figure 3.1. Southwest Afghanistan USMC Patrol Base showing Equipment Inventory, Source [1].

Sprague models this baseline grid with nine shelters, four generators, mean renewable energy production of 1.1 unit, and one battery storage with charge and discharge rate of 0.2 times battery capacity, respectively. The minimum allowable run and rest times for the generators are five minutes each, and all generators and renewable power are available to serve any of the shelters' cooling requirements. The actual minimum run and rest times for the generators are rounded up to six minutes because they must be multiples of the time step. More details on the inventory composition, equipment, storage, renewables, unmanaged demand, and uncertainty can be obtained from Chapter 5 of Sprague's thesis [1].

Tables 3.1 through 3.3 show the parameters for baseline shelter and generator configurations, as well as fuel consumption. We use the same mix of shelters and generators as in [1], although the identifying numbers for the shelters and the generators are slightly different.

Base Shelter Configurations				
Parameter	**Shelters 1-4, 7**	**Shelters 5, 6**	**Shelter 8**	**Shelter 9**
Usage	Billeting	Billeting	Billeting	COC
Type	Base-X 305	Base-X 305	Base-X 307	Base-X 307
Min. internal temp. [°F]	70	70	70	70
Max. internal temp. [°F]	80	80	80	80
ECU capacity [BTU/hr]	36,000	20,000	60,000	96,000
ECU power [kW]	4.5	1.6	8.5	13.0
Thermal slope [BTU/(hr.°C)]	-931	-931	-1,226	-1,254
Thermal intercept [BTU/hr]	37,790	37,790	48,794	60,454
ECU run / rest time [minutes]	2/2	2/2	2/2	2/2

Table 3.1. Model Baseline Shelter Configuration, Adapted from [1].

Baseline Generator Configurations				
Parameter	**Generator 1**	**Generator 2**	**Generator 3**	**Generator 4**
Type	AMMPS	AMMPS	AMMPS	AMMPS
Frequency [Hertz]	60	60	60	60
Rating [Kw]	10	30	60	10
Gen. run /rest time [minutes]	5 / 5	5 / 5	5 / 5	5 / 5

Table 3.2. Model Baseline Generator Configuration, Adapted from [1].

FUEL CONSUMPTION USING AVL					
Power Percent	Generator Model				
	5-kW	10-kW	15-kW	30-kW	60-kW
	gal/hr	gal/hr	gal/hr	gal/hr	gal/hr
110%	0.55	0.98	1.39	3.11	5.33
100%	0.51	0.88	1.24	2.79	4.92
75%	0.42	0.70	0.95	2.00	3.96
50%	0.34	0.53	0.73	1.39	2.74
25%	0.27	0.38	0.49	0.92	1.66
10%	0.23	0.29	0.38	0.65	1.08
0%	0.20	0.24	0.31	0.59	0.74

Table 3.3. AMMPS Generator Sets Fuel Consumption, Source [1].

3.2.2 Measures of Effectiveness

Our primary measure of effectiveness is cumulative fuel consumption. We examine this for both the RH-PFK and RH-U variants of the model, so another measure is the relative efficiency of RH-U to RH-PFK. We also look at the use of the generators, both in terms of total time, and the time operating at low efficiency. Additionally, we examine the temperature variation in each of the shelters in terms of the cooling performance of the ECUs. Both of our experiments assess these measures of effectiveness.

The baseline results in Sprague's thesis are illustrated using a single set of uncertain parameter data for his optimization model. We run multiple replications for a variety of different scenarios, chosen in structured ways, to provide new types of insight into the model's performance and robustness.

3.3 Experiment I: Baseline Scenario

This experiment analyzes Sprague's model and directly compares its results to his. It uses the same set of input parameters, including the number of shelters and the shelters' parameters, the same number of generators, and so on. Uncertainty implementation is also similar in that it includes the renewable power production, the unscheduled demand and the mean heat transfer intercept; the only difference is in the heat transfer intercept deviation, which is lower.

3.3.1 Factors

Table 3.4 displays the input factors that bring uncertainty into the model. For each distribution, we use the three parameters to generate independent sample data for time step 0 through time step 300. The "mean" represents the expected value. The "deviation" represents the half-width of a uniform distribution, expressed in terms of the proportion relative to a baseline value. In experiment I, the baseline value is the mean for all three sources of uncertainty.

Specifically, (3.1) shows the distribution of the unscheduled demand data at any given time step:

$$\begin{aligned}\text{Unscheduled}^{demand} \sim & \\ & \text{Unscheduled}^{mean} * \left(1 + \text{Uniform}\left[1 - \text{Unscheduled}^{dev}, \text{Unscheduled}^{dev}\right]\right).\end{aligned} \tag{3.1}$$

We only consider $\text{Unscheduled}^{dev} < 1$, so all generated values are greater than zero.

The heat transfer intercept is also uniformly distributed, as shown in (3.2).

$$\text{Intercept}^{transfer} \sim \text{Intercept}^{mean} * \left(\text{Uniform}\left[1 - \text{Intercept}^{dev}, 1 + \text{Intercept}^{dev}\right]\right). \tag{3.2}$$

Finally, the renewable production is uniformly distributed, as shown in (3.3).

$$\begin{aligned}\text{Renewable}^{production} \sim & \\ & \text{Renewable}^{mean} * \left(\text{Uniform}\left[1 - \text{Renewable}^{dev}, 1 + \text{Renewable}^{dev}\right]\right)\end{aligned} \tag{3.3}$$

3.3.2 Design

We construct an NOLH design [34], using an Excel spreadsheet template available at the Simulation Experiments and Efficient Designs (SEED) center website: https://harvest.nps.edu. Table 3.4 shows the uncertain factors and the ranges of values for each of the six factors. This design has 33 design points (i.e., combinations of factor settings), and can be used for up to eleven factors. The maximum pairwise correlation is 0.242. We ran five replications of the design. The results appear in Chapter 4.

Uncertain Factors		
Factor	**Type**	**Ranges**
Unscheduled mean	Continuous	[6.7, 9]
Unscheduled deviation	Continuous	[0.1, 0.2]
Renewable mean	Continuous	[0.9, 1.3]
Renewable deviation	Continuous	[0.1, 0.2]
Intercept mean	Continuous	[0.9, 1.1]
Intercept deviation	Continuous	[0.2, 0.5]

Table 3.4. Factors for Baseline Experiment.

3.4 Experiment II: Time-Varying Production and Demand

We add three additional factors to ensure our unscheduled demand and renewable production data reflect a more realistic pattern in an expeditionary power grid system. The factors for the heat transfer intercept remain unchanged. However, instead of holding the mean unscheduled demand constant during the entire period, we use three factors — the unscheduled base similar to unscheduled mean, the halfwidth used as the middle of the base, and offset used to control the peak height — to introduce a pattern that shows demand rising and falling during the course of the day. Similarly, we use three factors — a renewable magnitude multiplier, the halfwidth, and peak offset — to generate an expected mean renewable production that varies over the day. We use these factors to introduce a bell shaped pattern of a single cycle of a cosine function that accounts for the periods of zero to little demand and production, and periods of peak or high demand and production. We superimpose uniform noise, where the noise deviation is a factor (similar to experiment I). Figures 3.2 and 3.3 display examples of the trends and values we obtain. The trend in Figure 3.2 represents a more realistic depiction of the power grid system in which power demand rises gradually in the morning, peaks during the afternoon when the temperature rises and ECUs must provide more cooling, and drops eventually at night. Renewable production follows a very similar pattern of high solar energy production during daytime, bracketed by zero production at night.

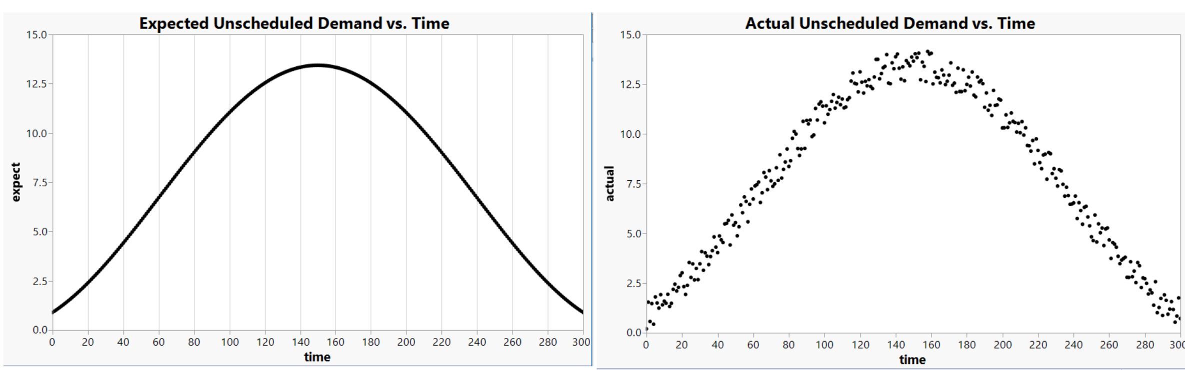

Figure 3.2. Example of Non-constant Unscheduled Demand Pattern, Experiment II .

To visually understand how this works, see the examples in Figures 3.3 and 3.2. We set the expected renewable energy to peak at 120, which represents the renewable offset, and set the halfwidth to 100, which means that the renewable drops down to zero at time 20 and

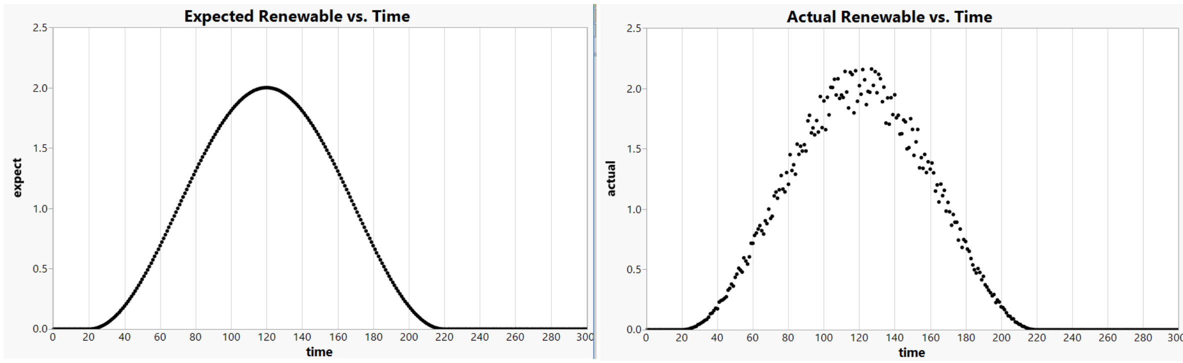

Figure 3.3. Example of Non-constant Renewable Energy Pattern, Experiment II.

time 220, as shown in Figure 3.3. The actual renewable production is set by superimposing a noise uniform random variation around the actual renewable to reflect the inconsistencies in renewable production. The peak of the expected renewable production in the left plot is equal to 2.0, representing a case where the renewable magnitude multiplier is 1.0. A larger value of the multiplier will result in a larger expected renewable production.

In Figure 3.2, we set the expected unscheduled demand at a halfwidth of 180, which ensures the unscheduled demand does not drop down to zero during the experiment. The actual unscheduled demand follows a similar pattern with a noise uniform random variation superimposed to reflect the unpredictability of unscheduled power demand.

3.4.1 Factors

The factor settings for this experiment are similar to those of experiment I, but now include the three new factors. Table 3.5 illustrates the factor settings. One other potential factor that we do not explore is the peak offset for the unscheduled demand curve; we keep it fixed at midday (time step 150), although this could be changed in future studies.

The ranges for the unscheduled halfwidth ensure that the mean unscheduled demand never falls to zero during our ten-hour day. In contrast, for the renewable production we explore combinations of halfwidths and offsets that can fall to zero at either or both ends of the day, or remain positive throughout the day. Consequently, we choose to vary the renewable magnitude multiplier, halfwidth, and deviation of the mean as separate factors, and let these determine the total renewable production. We describe our process for using these factors

Uncertain Factors			
Factor	**Type**	**Ranges**	**Remarks**
Unscheduled base	Continuous	[6.7, 9]	Similar to the unscheduled mean
Unscheduled halfwidth	Integer	[180, 300]	Halfwidth used to control the load peak
Unscheduled deviation noise	Continuous	[0.1, 0.2]	Similar to the unscheduled deviation
Renewable magnitude	Continuous	[9, 13]	Multiplier for the renewable
Renewable mean halfwidth	Integer	[90, 210]	Halfwidth used to control production drop-off times
Renewable deviation noise	Continuous	[0.1, 0.2]	Similar to renewable deviation
Renewable peak offset	Integer	[120, 180]	Also used to control production drop-off times
Intercept mean	Continuous	[0.9, 1.1]	Same as experiment I
Intercept deviation	Continuous	[0.01, 0.025]	Same as experiment I

Table 3.5. Factors for Secondary Experiment.

as well as demonstrate pictorially in Section 3.4. Figures 3.4 and 3.5 show additional illustrations of how the factors were used.

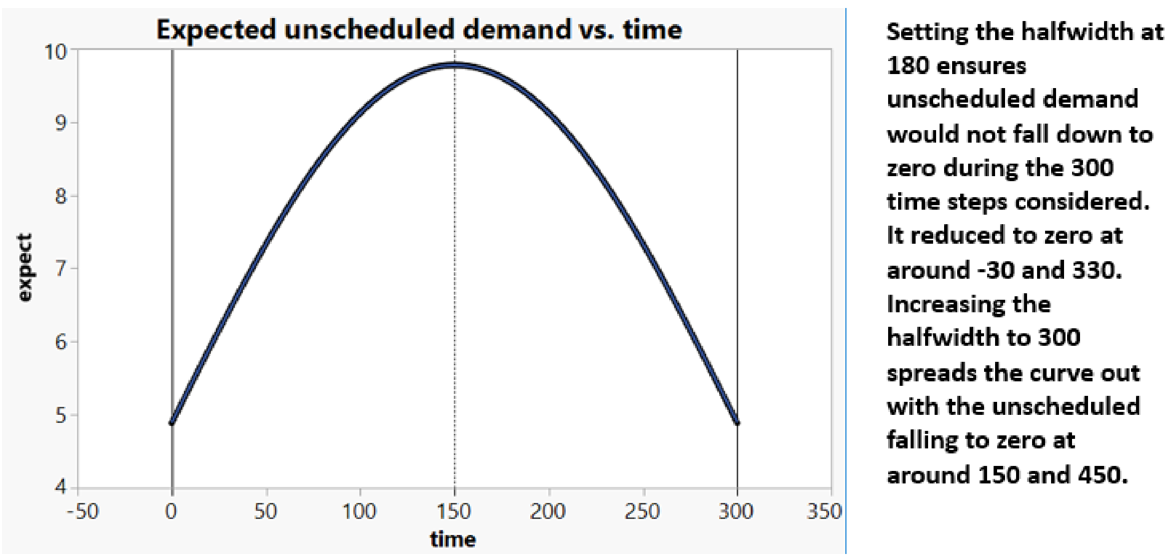

Figure 3.4. Non-constant Unscheduled Demand Illustration, Experiment II.

3.4.2 Design

The NOLH design setup for the second experiment resembles the first experiment, except for the addition of the three new factors. The maximum pairwise correlation is 0.0234. We ran five replications of the experiments, and the analysis of the results appears in Chapter 4.

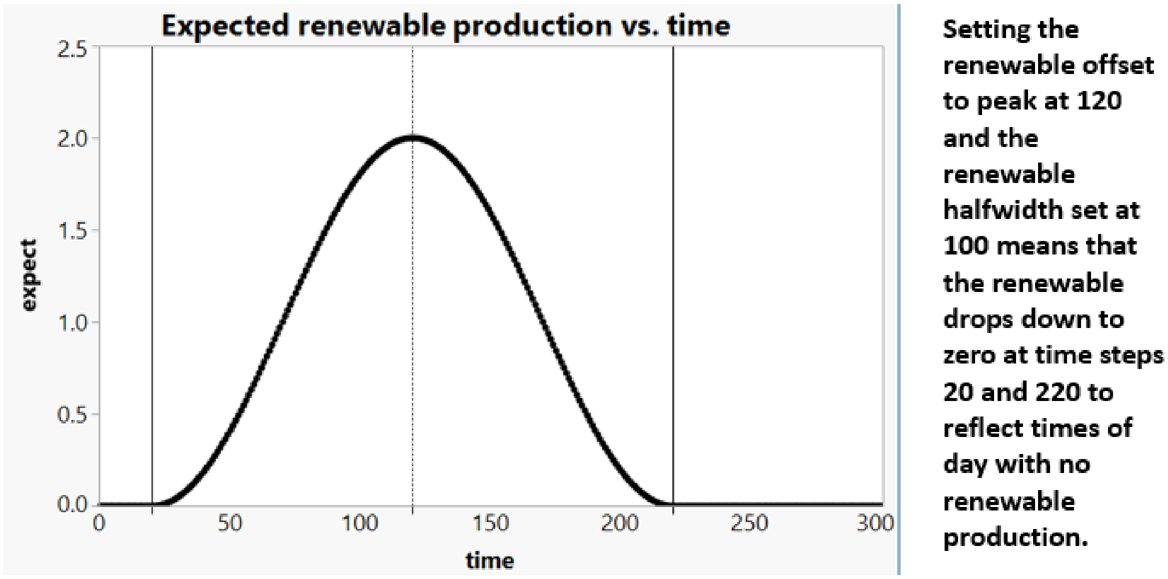

Figure 3.5. Non-constant Renewable Energy Illustration, Experiment II.

3.5 Summary

We conduct two experiments using two 33-design point NOLHs to determine which of the uncertain factors most affect overall fuel consumption. These factors include the unscheduled demand requirements, the renewable energy production, and the heat transfer intercept.

THIS PAGE INTENTIONALLY LEFT BLANK

CHAPTER 4:
Analysis of Results

We now present the results of our experiments, including the summary outcomes of Sprague's model as well as the results from our DOE. Our baseline scenario with experiment I uses the same configuration as Sprague's with the exception of a smaller intercept deviation factor value, so we compare the results obtained directly with Sprague's in this DOE analysis.

Also, we analyze the experimental data to gain additional insight into the behavior of the model, the uncertain input parameters, their relationships and interactions, and their influence on the cumulative total fuel consumption.

4.1 Model Results

As previously discussed, Sprague's model minimizes fuel consumption by optimally scheduling which of the four generators and nine ECUs to operate, while maintaining the shelter's internal temperature within the specified limit. The model results include the cumulative total fuel consumption, the generators' operation schedule, and the ECUs operation schedule.

4.1.1 Model Fuel Consumption Results

Sprague uses the legacy system (LGCY) model variant as the baseline or the standard to measure model improvements. The LGCY allows the generators to run continuously without managing any resources, ensuring enough power to support all the connected loads [1]. It implements a simple threshold policy for the ECUs, turning on each ECU when its shelter hits an upper temperature limit and turning it off when the shelter's temperature reaches a lower limit. Table 4.1 shows the cumulative fuel consumption of Sprague's model for three model variants: the LGCY used as the baseline, the RH-PFK and the RH-U, over a 10-hour optimization horizon. We also introduce a relative efficiency measure to compare the performance of the two model variants, RH-PFK and RH-U, that are the focus of this study. We compute this parameter as the ratio of cumulative total fuel for the RH-U to that

of the RH-PFK. Any time the relative efficiency is greater than one, the RH-PFK performs better. As expected, the results show that the LGCY model consumes the most fuel [1]. The RH-PFK and the RH-U record substantial improvements over the LGCY variant [1].

Baseline Cumulative Fuel Consumption - 10 hours				
Variant	Best Solution [gallons]	Best Possible [gallons]	Reduction vs. LGCY [%]	Relative Efficiency vs. RH-PFK Best Possible
LGCY	32.9	32.9	NA	1.44
RH - PFK	22.9	22.9	30.4	NA
RH - U	23.7	23.5	28	1.02

Table 4.1. Baseline Configuration Cumulative Fuel Consumption, Adapted from [1].

Design point 17 from our DOE experiment I closely resembles the single run in Sprague's baseline. Not only is the baseline scenario the same, but so are the values of the unscheduled mean, the renewable mean, and the intercept mean. Specific values for the actual demand differ from those of Sprague, but generating the actual unscheduled demand and the actual renewable production requires using identical distributions. The only difference is that we use a narrower distribution for generating the actual intercept values: Sprague uses an intercept deviation of 0.05, while we use a value of 0.02. The values of a comparison of the cumulative fuel consumption results obtained from our experiment's five replications are similar to those of Sprague. The values of RH-PFK range from 22.00 to 22.42, the values of RH-U range from 22.13 to 23.51, and the relative efficiency ranges from 0.55 to 2.50. Overall, the average cumulative fuel consumption of approximately 22.9 gallons for RH-U and 22.2 gallons for RH-PFK is only about 3.5% more fuel consumption for the RH-U as reported by Sprague.

4.2 DOE Results

The model results from General Algebraic Modeling System (GAMS) provide a substantial amount of information spread across multiple files. We use JMP Pro Version 12.0.1 to filter, consolidate, organize, and process our data into a format that can be easily analyzed [35].

4.2.1 Initial Exploration of Experimental Data

We first examine a subset of our data set at time step 300 to obtain cumulative fuel consumption at the end of the time steps for each model run and each design point.

Figures 4.1 and 4.2 demonstrate that this subset of the relative efficiency distribution has outliers. Further investigation reveals that the outliers resulted from infeasible solutions obtained by the model run for some design points, although no design point yields infeasible solutions for more than two of its five replications. One potential explanation is that occasionally, the optimization solver "times out" on a particular iteration based on the tolerance time limit set for the model. This can lead to an infeasible solution for subsequent iterations of the rolling horizon algorithm. The time limit set for the model in each iteration of the rolling horizon algorithm is 3,600 seconds. The overall completion times for all iterations vary widely in our experiments, from 1,953 seconds to 10,757 seconds.

If Sprague's model is to be used in actual operations, then this infeasibility requires further investigation. A larger number of replications would provide more insight into the proportion of time the optimization model is unable to find a feasible solution in a timely manner. A major advantage of using DOE to study systems or models is its ability to vary factors simultaneously and gain insights not obtainable from varying such factors one at a time. This means that if certain factors or factor combinations contribute to the chances of obtaining feasible solutions, the DOE may help identify them.

We exclude outliers from further consideration in our analysis, and the relative efficiency distributions without outliers appear in Figures 4.3 and 4.4. As expected, RH-PFK consistently outperforms RH-U, by up to 8% in experiment I and up to 14% in experiment II, as shown in Figures 4.3 and 4.4. On average, RH-PFK outperforms RH-U by 2.8% for experiment I. Therefore, the results are consistent with Sprague's conclusion that uncertainty increases the fuel consumption only slightly. Our experiment validates that this performance holds whenever a solution is obtainable, and does so across multiple replications for all design points. For experiment II, RH-PFK outperforms RH-U, on average, by 5.1%.

4.2.2 Generator Behavior Insights

We are interested in the uncertain factors' influence on the cumulative total fuel consumption as well as the behavior of other model responses. The generators' operation and load factor

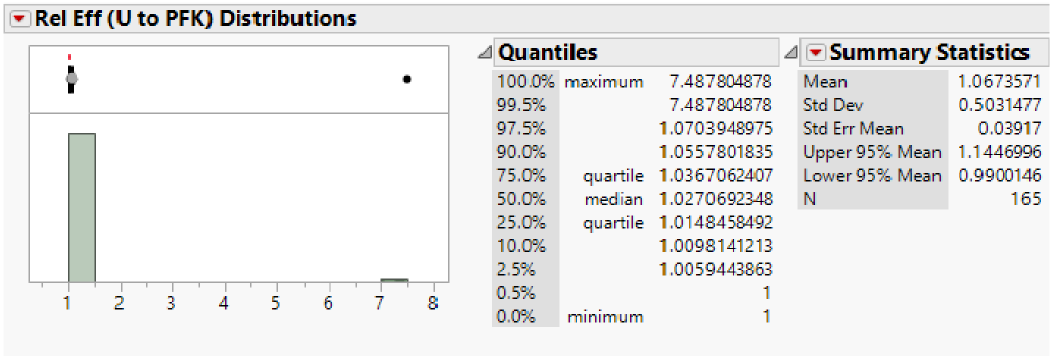

100.0%	maximum	7.487804878
99.5%		7.487804878
97.5%		1.0703948975
90.0%		1.0557801835
75.0%	quartile	1.0367062407
50.0%	median	1.0270692348
25.0%	quartile	1.0148458492
10.0%		1.0098141213
2.5%		1.0059443863
0.5%		1
0.0%	minimum	1

Mean	1.0673571
Std Dev	0.5031477
Std Err Mean	0.03917
Upper 95% Mean	1.1446996
Lower 95% Mean	0.9900146
N	165

Figure 4.1. Experiment I Time Step 300 Relative Efficiency Distribution With Outlier.

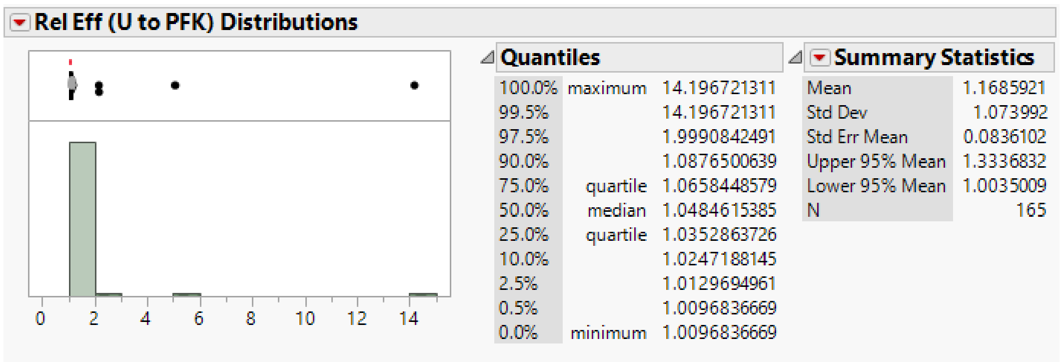

100.0%	maximum	14.196721311
99.5%		14.196721311
97.5%		1.9990842491
90.0%		1.0876500639
75.0%	quartile	1.0658448579
50.0%	median	1.0484615385
25.0%	quartile	1.0352863726
10.0%		1.0247188145
2.5%		1.0129694961
0.5%		1.0096836669
0.0%	minimum	1.0096836669

Mean	1.1685921
Std Dev	1.073992
Std Err Mean	0.0836102
Upper 95% Mean	1.3336832
Lower 95% Mean	1.0035009
N	165

Figure 4.2. Experiment II Time Step 300 Relative Efficiency Distribution With Outlier.

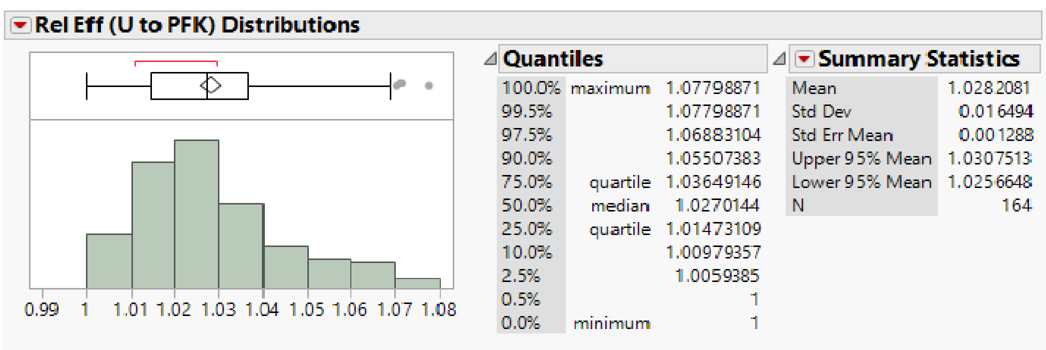

100.0%	maximum	1.07798871
99.5%		1.07798871
97.5%		1.06883104
90.0%		1.05507383
75.0%	quartile	1.03649146
50.0%	median	1.0270144
25.0%	quartile	1.01473109
10.0%		1.00979357
2.5%		1.0059385
0.5%		1
0.0%	minimum	1

Mean	1.0282081
Std Dev	0.016494
Std Err Mean	0.001288
Upper 95% Mean	1.0307513
Lower 95% Mean	1.0256648
N	164

Figure 4.3. Experiment I Time Step 300 Relative Efficiency Distribution Without Outlier.

affect overall fuel consumption, and a closer look at these may help to obtain useful insights

Rel Eff (U to PFK) Distributions

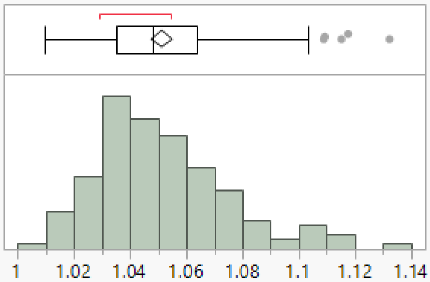

Quantiles

100.0%	maximum	1.1324786325
99.5%		1.1324786325
97.5%		1.1150037667
90.0%		1.0834770563
75.0%	quartile	1.0639902426
50.0%	median	1.0477941176
25.0%	quartile	1.0348962524
10.0%		1.0241274553
2.5%		1.0129634564
0.5%		1.0096836669
0.0%	minimum	1.0096836669

Summary Statistics

Mean	1.0512081
Std Dev	0.0236721
Std Err Mean	0.0018656
Upper 95% Mean	1.0548925
Lower 95% Mean	1.0475237
N	161

Figure 4.4. Experiment II Time Step 300 Relative Efficiency Distribution Without Outlier.

into the generators' behavior in the model. The GAMS output already includes each generator's status and load factor during operation, for every time step. Each generator has two levels representing its status: zero when idle and one when running. Each generator's load factor is also represented by a continuous variable between zero and one. From these variables, we can compute the number of generators operating at every time step. We can also obtain insights into the proportion of time each generator operates, the proportion of time that specific numbers of generators are turned on during the optimization, and the proportion of time generators operate below or above a load factor performance level.

4.2.3 Experiment I

Using the results of experiment I, we begin by analyzing the uncertain factors' influence on the cumulative total fuel consumption using the partition tree method. Partition trees tease apart relationships between response variables and the predictor variables by recursively splitting the data set where relationships occur, thereby creating a tree-like structure. The heat transfer intercept mean multiplier of the thermal model is the only influencing factor after three splits for both the RH-PFK and the RH-U model variants, yielding RSquare values of 0.94 and 0.93, respectively. Figures 4.5 and 4.6 display the results. RSquare is a statistical measure that helps to determine the proportion of variance in our response factor, or the cumulative total fuel, which can be explained or predicted by the predictor factors, or the uncertain factors. It is not surprising that the partition tree results are nearly identical for the two model variants, because the correlation between the two performance measures is nearly 100% (0.99). The influence of other uncertain factors is minimal in this experiment

since at least 93% of the variation could be explained by the intercept mean alone. We conclude that the heat transfer factor (the intercept mean multiplier), has the most influence on the fuel consumption of the factors we tested and subject to the degree of variability. A higher heat transfer intercept means that more fuel is used. For instance, if there are different types of shelters available, selecting those with lower heat transfer intercepts to reduce fuel consumption. Of course, operational considerations may also constrain the choices.

RSquare	RMSE	N	Number of Splits	AICc
0.939	0.5658331	164	3	289.01

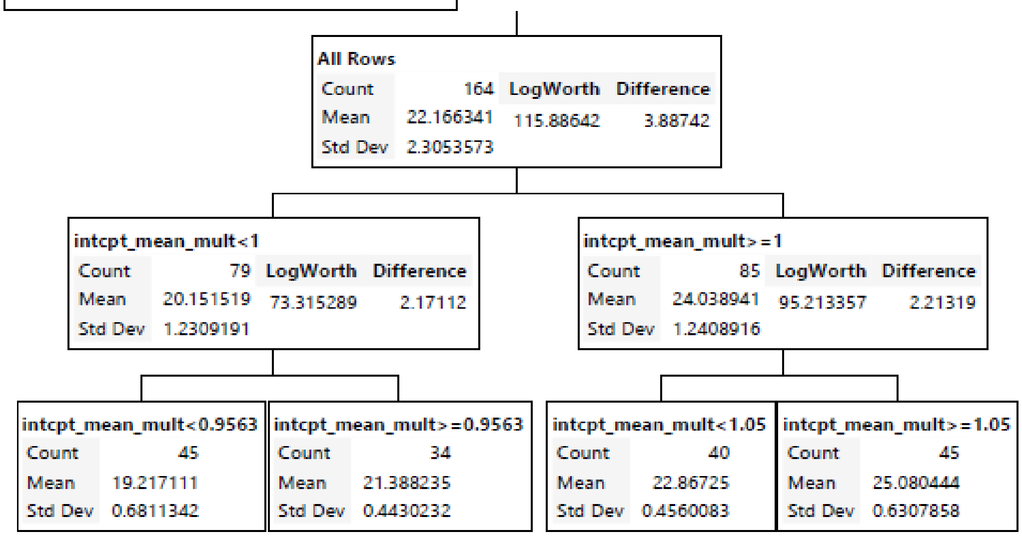

Figure 4.5. Experiment I Factors' Influence on Cumulative Total Fuel Partition Tree, RH-PFK.

Furthermore, we apply a linear regression approach to fit a model for the cumulative total fuel, by allowing stepwise regression to select among the main effects, quadratic effects, and two-way interactions. This approach helps to investigate the type of relationship that exists between our response factor and the predictor factors. Figures 4.7 and 4.8 show the results. The outcomes parallel those of the partition tree approach for both model variants, but also reveal that the relationship between each of the important factors and fuel used is linear. The intercept mean dominates other factors, followed by the unscheduled mean, and the renewable mean, in that order. Once again, the intercept mean could explain at least 92% of the variation in our response factor. The side-by-side plots in Figures 4.7 and

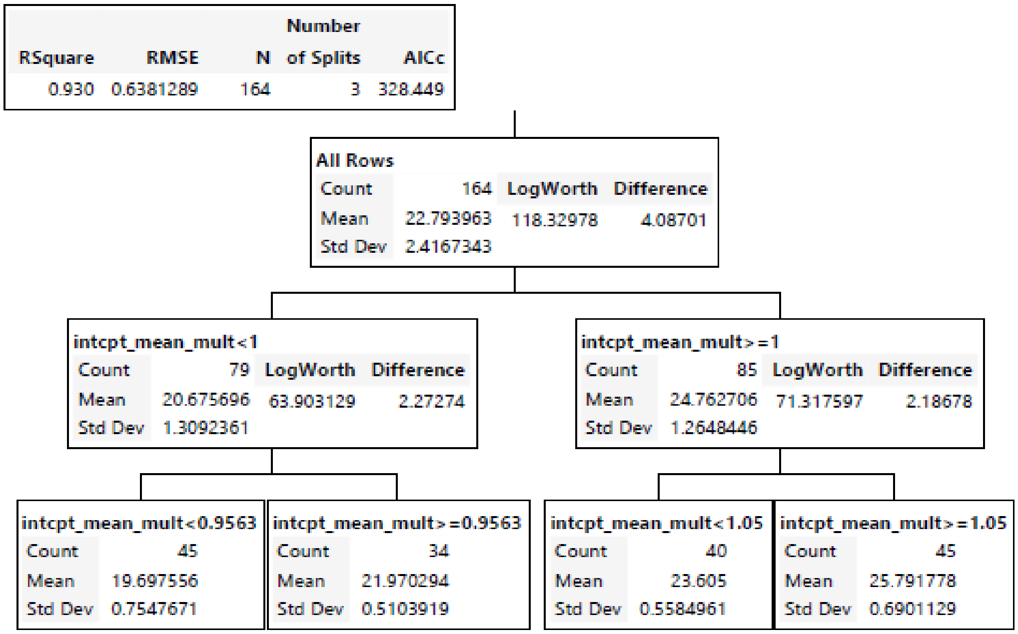

Figure 4.6. Experiment I Factors' Influence on Cumulative Total Fuel Partition Tree, RH-U.

4.8 highlight the difference in the RSquare value when we use one dominant factor as a predictor versus three significant factors. We conclude that the heat transfer intercept mean contributes the most to cumulative fuel consumption in the Sprague model's approximation of the expeditionary power grid. However, the majority of the power production capacity for the grid comes from the generator in Sprague's model. Consequently, the renewable production would likely be more influential if it were represented by a larger proportion of the production capacity.

Practically, decision makers need to invest in better shelter structures with reduced heat absorption properties, as well as develop control measures that prevent heat transfer to the shelters to reduce fuel consumption. Measures such as controlling cooling boundaries that ensure individuals transiting shelters close the doors plays an important role in reducing fuel consumption. None of the other uncertainty factors has any major influence on the fuel consumption because the majority of the power generation is from the generator, and (as we shall discuss shortly) the unscheduled demand is not putting any major stress on the power

grid. Thus, the optimization model can handle that amount of uncertainty explored in the DOE whenever it could find a feasible solution.

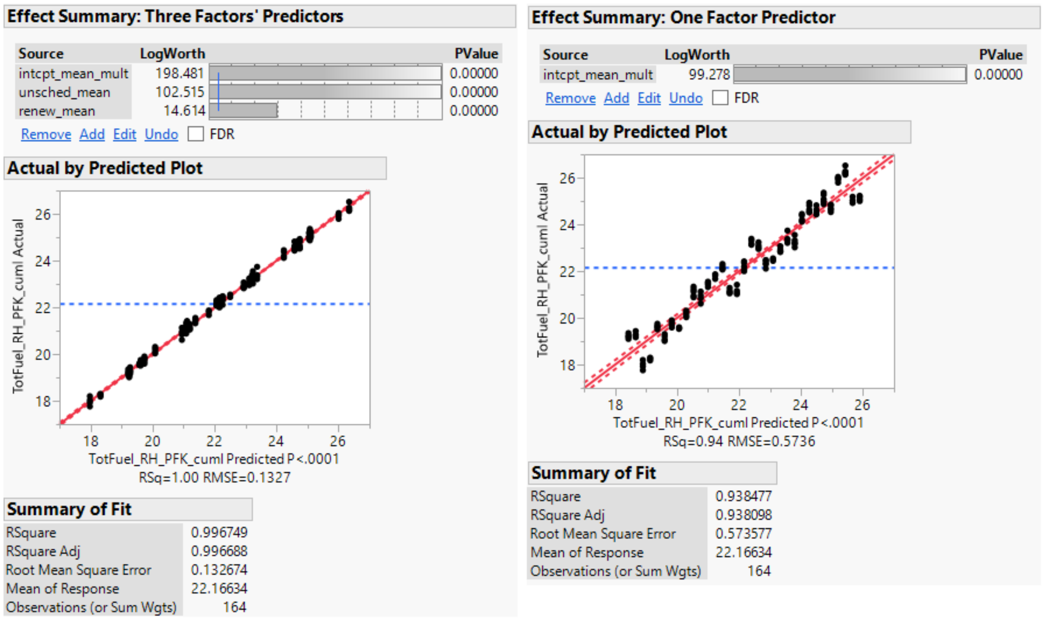

Figure 4.7. Experiment I Factors' Influence on Cumulative Total Fuel Stepwise Regression, RH-PFK.

Additionally, we examine the generators' behavior in the model to obtain some insights on use and performance. Table 4.2 shows the proportion of time each generator operates. Both model variants use the 10 kW generators, generators 1 and 4, about the same amount of time (about 34% for RH-PFK and about 33% for RH-U). The range of use for both generators is also about the same. It appears that the model uses smaller capacity generators to handle loads first, then turns on the larger generators if the smaller ones cannot handle the load. This is expected since larger generators are less efficient when operating at low loads. We conclude that the model performs well in managing fuel efficiency by matching load requirements with smaller generators first and then using larger ones when the load requirement exceeds their capacity. Generator 2 is the least used for both model variants at about 17%.

Also, the proportion of the number of generators turned on, as shown in Table 4.3, suggests that the model rarely requires more than two generators at any point. A single generator operates approximately 69% of the time for RH-PFK and approximately 70% of the time for

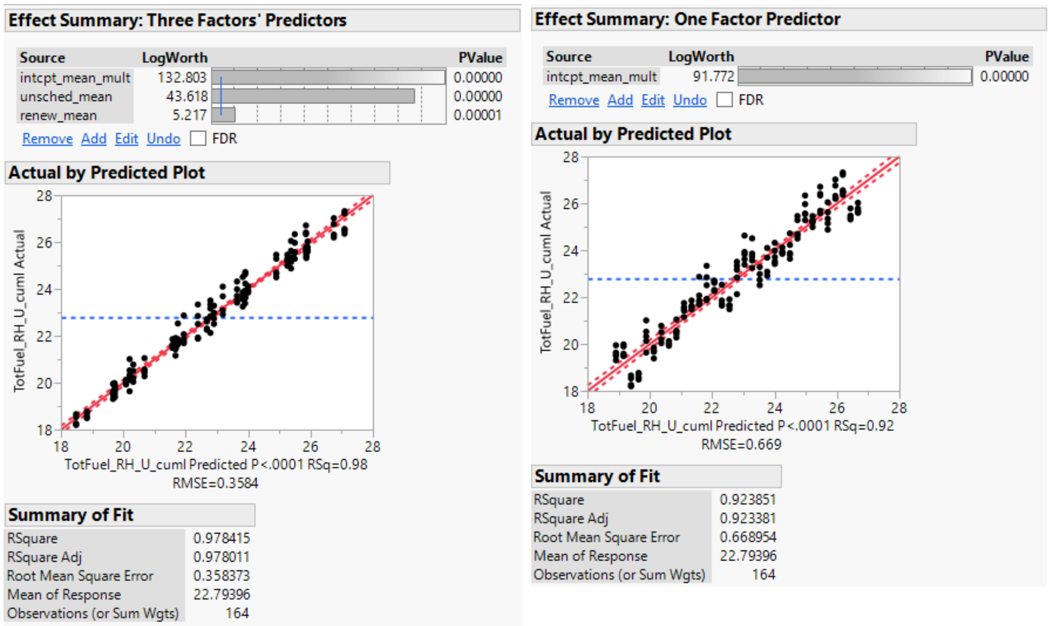

Figure 4.8. Experiment I Factors' Influence on Cumulative Total Fuel Stepwise Linear Regression, RH-U.

Proportion of Time Generator Operates				
	RH-PFK		RH-U	
Generator	Proportion in %	Range	Proportion in %	Range
1 (10kW)	34.76	23.59 - 48.17	33.07	17.28 - 46.84
2 (30kW)	17.44	7.64 - 32.89	17.58	8.64 - 31.23
3 (60kW)	39.35	24.92 - 51.50	47.17	29.90 - 61.13
4 (10kW)	34.30	22.59 - 50.50	32.92	22.59 - 48.17

Table 4.2. Experiment I Proportion of Time Each Generator Operates, RH-PFK vs. RH-U.

RH-U. The results display that the power grid's need for four generators at any point in time is almost zero. Further studies need to investigate whether the power grid can efficiently operate with fewer generators and still be fuel efficient.

Lastly, we analyze the load factor performance of the generators as shown in Figures 4.9 and 4.10. The quantile summary statistic reveals that 75% of the operating loads of the small generators (generators 1 and 4) are at least an 85% load factor for the RH-PFK. This result indicates that, when used, these two generators operate at a high load factor which reduces fuel consumption. The situation is similar for the RH-U when 50% of generators 1 and 4's

Proportion Number of Generators Turned On				
	RH-PFK		RH-U	
No of Generator	Proportion in %	Range	Proportion in %	Range
0	3.24	0.33 -8.97	0.92	0.00 - 4.65
1	68.93	55.81 - 79.07	69.63	56.48 - 83.06
2	26.60	15.61 - 40.53	27.29	16.28 - 39.20
3	1.20	0.00 - 4.32	2.13	0.00 - 7.97
4	0.03	0.00 - 0.99	0.04	0.00 - 0.99

Table 4.3. Experiment I Proportion of The Number of Generators Turned-On Every Time-Step, RH-PFK vs. RH-U

loads are at least an 81% load factor. This difference exhibits that generator 3's load factor is not as good as generators 1 and 4's load factors, particularly for RH-U. We conclude that a further experiment could vary the number and capabilities of the available generators in order to see whether different configurations result in better load factors, while still meeting the demand. Realistically, the installation of the right combination of generator ratings improves power grid load factor efficiency, which directly translates into fuel savings.

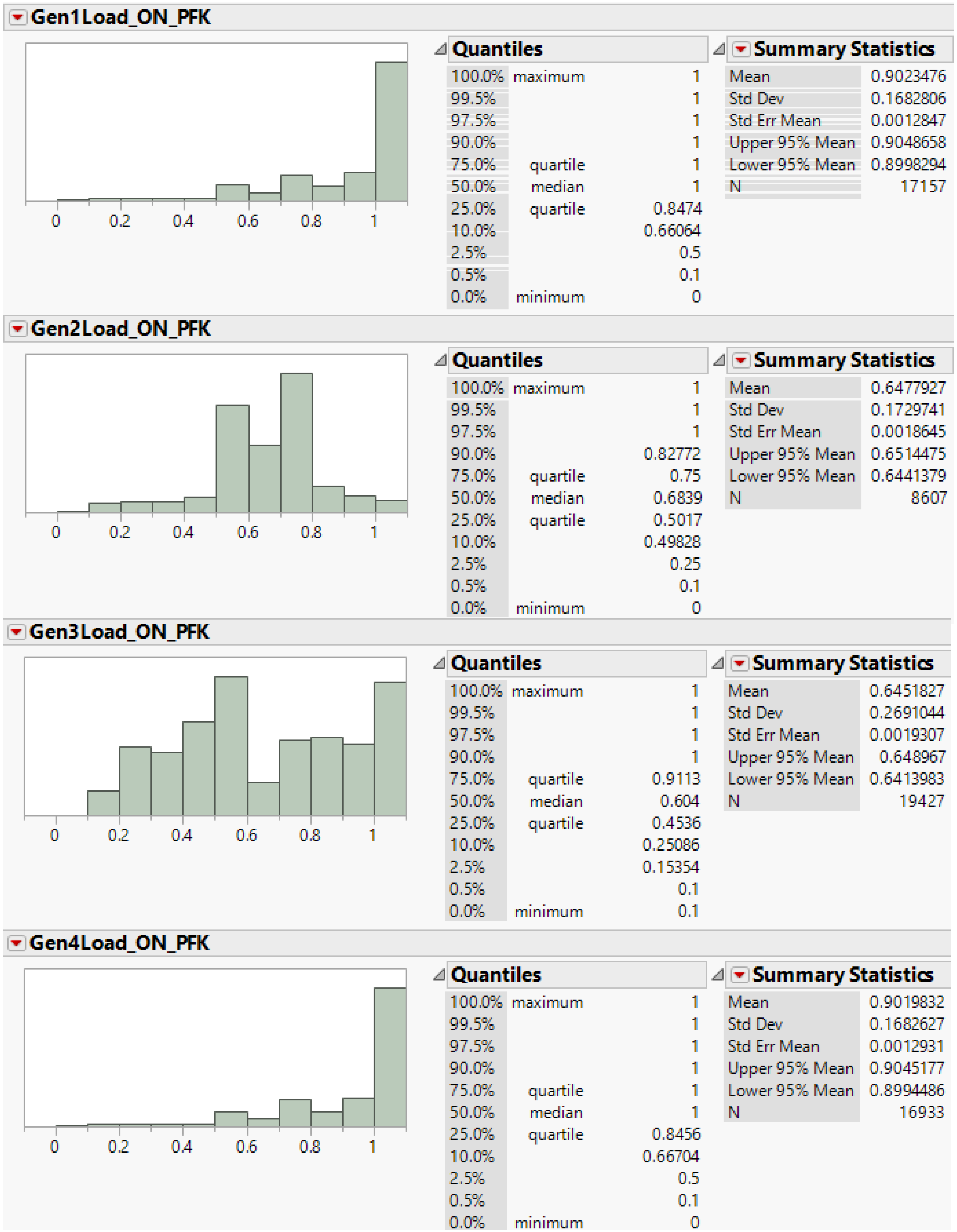

Figure 4.9. Experiment I Distribution of Generators' Load during Operation, RH-PFK.

Gen1Load_ON_U

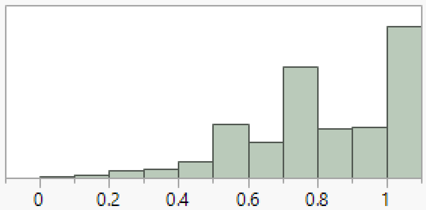

Quantiles

100.0%	maximum	1
99.5%		1
97.5%		1
90.0%		1
75.0%	quartile	1
50.0%	median	0.8184
25.0%	quartile	0.6981
10.0%		0.5
2.5%		0.3489
0.5%		0.1661375
0.0%	minimum	0

Summary Statistics

Mean	0.8003247
Std Dev	0.2005776
Std Err Mean	0.0015699
Upper 95% Mean	0.8034019
Lower 95% Mean	0.7972476
N	16324

Gen2Load_ON_U

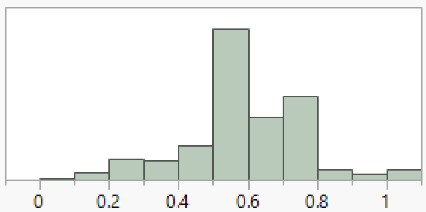

Quantiles

100.0%	maximum	1
99.5%		1
97.5%		0.97329
90.0%		0.75
75.0%	quartile	0.715075
50.0%	median	0.5406
25.0%	quartile	0.5
10.0%		0.37104
2.5%		0.246525
0.5%		0.1
0.0%	minimum	0

Summary Statistics

Mean	0.5757252
Std Dev	0.1693349
Std Err Mean	0.0018176
Upper 95% Mean	0.5792881
Lower 95% Mean	0.5721624
N	8680

Gen3Load_ON_U

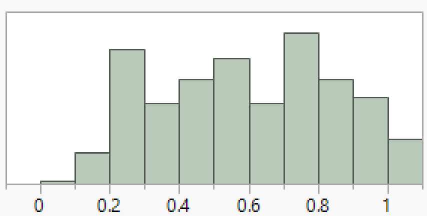

Quantiles

100.0%	maximum	1
99.5%		1
97.5%		1
90.0%		0.9464
75.0%	quartile	0.7991
50.0%	median	0.5893
25.0%	quartile	0.3906
10.0%		0.25
2.5%		0.15566
0.5%		0.1
0.0%	minimum	0

Summary Statistics

Mean	0.592607
Std Dev	0.2515727
Std Err Mean	0.0016487
Upper 95% Mean	0.5958386
Lower 95% Mean	0.5893754
N	23283

Gen4Load_ON_U

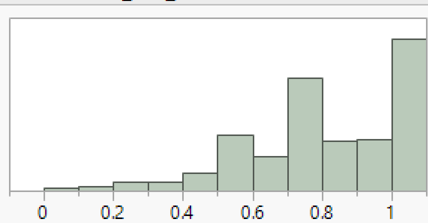

Quantiles

100.0%	maximum	1
99.5%		1
97.5%		1
90.0%		1
75.0%	quartile	1
50.0%	median	0.8134
25.0%	quartile	0.694725
10.0%		0.5
2.5%		0.3027225

Summary Statistics

Mean	0.7960542
Std Dev	0.2057428
Std Err Mean	0.0016139
Upper 95% Mean	0.7992175
Lower 95% Mean	0.7928908
N	16252

Figure 4.10. Experiment I Distribution of Generators' Load during Operation, RH-U.

4.2.4 Experiment II

This experiment introduces more realistic unscheduled demands and renewable production data into our analysis. Also, the experiment incorporates a larger amount of renewable energy production into the grid. We employ the same evaluation approach as for experiment I.

Once again, in a few cases the model does not report a feasible solution for the RH-PFK (specifically, one replication for design points 2 and 13, and two replications for design point 6). We omit the infeasible replications in the analyses that follow. We analyze the uncertain factors' influence on the cumulative total fuel consumption using a partition tree. The expected intercept and the renewable halfwidth with the RSquare value of 0.80 are the only influencing factors after three splits for the RH-PFK. However, for the RH-U model variant, the influencing factors are the renewable halfwidth, the expected intercept, and the renewable noise deviation with an RSquare value of 0.66. Figures 4.11 and 4.12 display the results. The difference in outcomes from the experiment I results signifies that the grid configuration, demand patterns, and renewable production pattern have a definite impact on fuel consumption. Additionally, we see that fuel consumption savings result if we increase renewable energy production on the power grid.

In addition, we use stepwise linear regression to fit a model for the cumulative total fuel at time step 300, allowing for main effects, quadratic effects, and two-way interactions. This approach helps to uncover the type of relationship that exists between our predictor factors and this response. Figures 4.13 and 4.14 show that simple relationships perform well for both of the optimization model variants. For both model variants, the influencing factors include the expected intercept, the renewable halfwidth, renewable magnitude multiplier, and the unscheduled base. RH-PFK recorded a RSquare value of 0.99 and RH-U also documented a RSquare value of 0.99, an indication that almost 100% of the variation in the cumulative total fuel could be attributed to these influencing factors. This experiment II outcome highlights the importance of the proportion of power production from various energy sources in grid power generation capacity. This outcome also shows that the uncertainty of the renewable production has greater influence than other sources of uncertainty for the factor ranges we investigate. The signs of the coefficients make sense. For instance, more fuel is used when the expected intercept increases while less fuel is consumed as we increase the renewable halfwidth. This implies that if we have a higher peak renewable production, we end up not using the generator as much which translates into reduced fuel consumption.

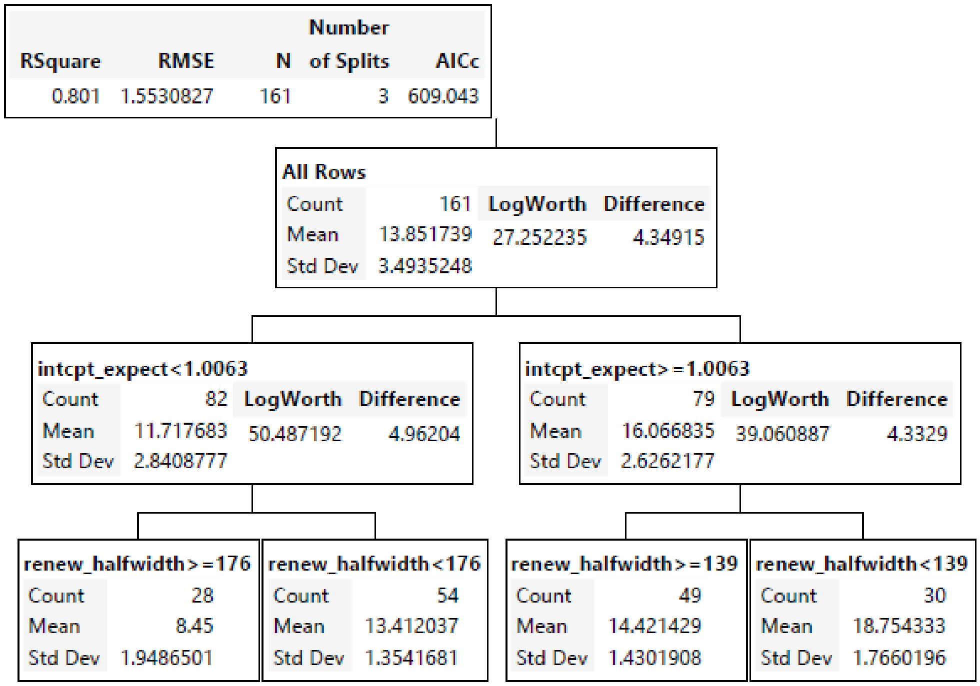

Figure 4.11. Experiment II Factors' Influence on Cumulative Total Fuel Partition Tree, RH-PFK.

Furthermore, we look into the generators' behavior to obtain useful insights on performance and utilization. Table 4.4 exhibits the proportion of time each generator operates. Generators 1 and 4, both with power ratings of 10 kW ran the most in the RH-PFK model variant. The model used both generators approximately 28% of the time. They also manifested about the same range of use observed in experiment I. We can conclude that the model is doing what is expected by using smaller generators first to take advantage of better load factor for fuel efficiency, which is similar to the results of the first experiment. Generators 1, 3, and 4, with power ratings of 10 kW, 60 kW, and 10 kW, respectively, are the most utilized by the RH-U model variant. All three generators ran approximately 30% of the time. On the other hand, generator 2 with a power rating of 30 kW ran the least for both model variants, or approximately 16% of the time. This result is consistent with our findings from experiment I, and we conclude that this generator's use requires more investigation as to whether a smaller generator with a better load factor could obtain better fuel efficiency.

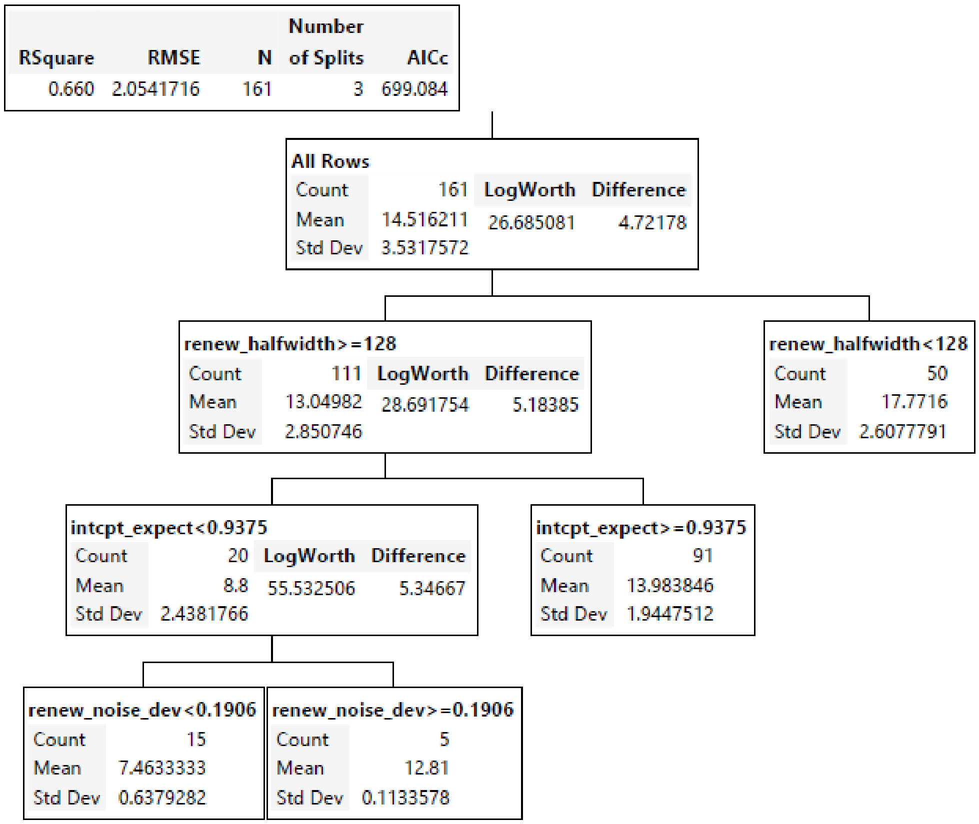

Figure 4.12. Experiment II Factors' Influence on Cumulative Total Fuel Partition Tree, RH-U.

Proportion of Time Generator Operates				
	RH-PFK		RH-U	
Generator	**Proportion in %**	**Range**	**Proportion in %**	**Range**
1 (10kW)	28.01	12.29 - 43.19	29.99	15.95 - 44.52
2 (30kW)	16.26	3.99 - 36.54	15.95	5.32 - 30.23
3 (60kW)	22.50	0.00 - 42.19	30.75	1.99 - 55.15
4 (10kW)	27.86	15.61 - 45.18	30.03	17.28 - 45.85

Table 4.4. Experiment II Proportion of Time Each Generator Operates, RH-PFK vs. RH-U.

Similarly, Table 4.5 reveals that the model rarely requires more than two generators to be turned on at any point. Approximately one generator operates 62% of the time for RH-PFK and approximately 66% of the time for RH-U. The results show that the power grid almost never requires simultaneous use of three or four generators at any point, which validates our

Effect Summary

Source	LogWorth	PValue
intcpt_expect	146.921	0.00000
renew_halfwidth	138.826	0.00000
renew_mag_mult	90.052	0.00000
unsched_base	58.395	0.00000

Remove Add Edit Undo FDR

Actual by Predicted Plot

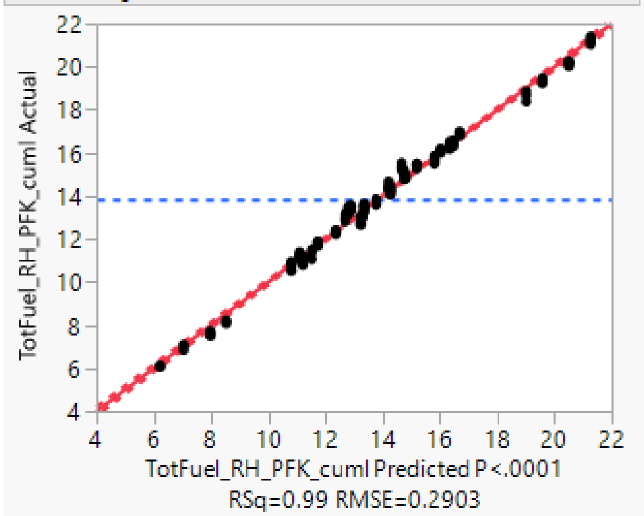

Summary of Fit

RSquare	0.993269
RSquare Adj	0.993097
Root Mean Square Error	0.290263
Mean of Response	13.85174
Observations (or Sum Wgts)	161

Parameter Estimates

Term	Estimate	Std Error	t Ratio	Prob>|t|
Intercept	-15.00064	0.523792	-28.64	<.0001*
renew_mag_mult	-0.867232	0.019419	-44.66	<.0001*
intcpt_expect	40.522756	0.380139	106.60	<.0001*
unsched_base	0.8770169	0.033404	26.25	<.0001*
renew_halfwidth	-0.060631	0.000642	-94.42	<.0001*

Figure 4.13. Experiment II Factors' Influence on Cumulative Total Fuel Stepwise Regression, RH-PFK.

earlier finding in experiment I. The power grid may operate efficiently with fewer generators. This suggestion requires further studies to confirm the feasibility in support of fuel savings.

Effect Summary

Source	LogWorth	PValue
intcpt_expect	128.796	0.00000
renew_halfwidth	122.000	0.00000
renew_mag_mult	70.498	0.00000
unsched_base	45.251	0.00000

Remove Add Edit Undo FDR

Actual by Predicted Plot

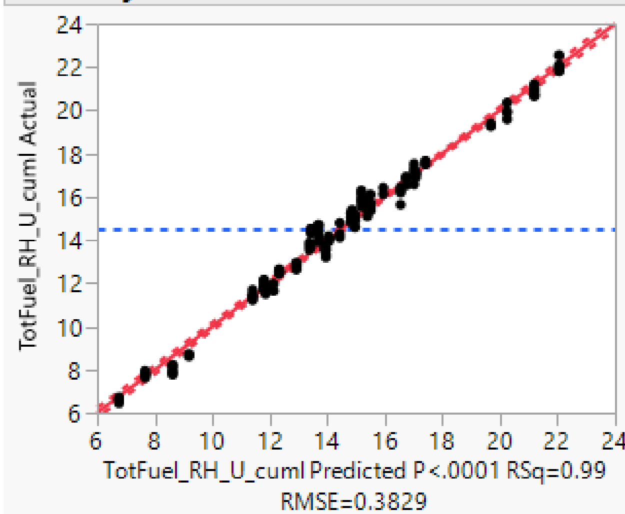

Summary of Fit

RSquare	0.988542
RSquare Adj	0.988248
Root Mean Square Error	0.382863
Mean of Response	14.51621
Observations (or Sum Wgts)	161

Parameter Estimates

Term	Estimate	Std Error	t Ratio	Prob>|t|
Intercept	-14.89622	0.690893	-21.56	<.0001*
renew_mag_mult	-0.830706	0.025614	-32.43	<.0001*
intcpt_expect	40.706239	0.501411	81.18	<.0001*
unsched_base	0.9006767	0.044061	20.44	<.0001*
renew_halfwidth	-0.062036	0.000847	-73.24	<.0001*

Figure 4.14. Experiment II Factors' Influence on Cumulative Total Fuel Stepwise Linear Regression, RH-U.

Lastly, Figures 4.15 and 4.16 demonstrate our analysis of the load factor performance of the generators. The quantile summary statistic reveals that 75% of generators 1 and 4's loads have at least an 81% load factor for the RH-PFK which indicates that, when used, these

Proportion Number of Generators Turned On				
	RH-PFK		RH-U	
No of Generator	Proportion in %	Range	Proportion in %	Range
0	21.79	5.65 - 47.84	13.82	1.99 - 33.22
1	62.10	43.85 - 76.74	66.26	52.82 - 75.42
2	15.78	2.99 - 33.89	19.08	8.97 - 32.89
3	0.32	0.00 - 2.66	0.60	0.00 - 3.32
4	0.004	0.00 - 0.33	0.008	0.00 - 0.66

Table 4.5. Experiment II Proportion of The Number of Generators Turned On At Every Time-Step, RH-PFK vs. RH-U.

two generators operate at a high load factor that reduces fuel consumption. The situation is similar to the RH-U when 50% of generators 1 and 4's loads have at least a 75% load factor. Generators 1 and 4 run the most for RH-PFK, and they have the best load factor as well, which is good for the power grid fuel consumption savings. However, the situation differs for the RH-U when generators 1, 3, and 4 display almost the same amount of usage, but with only 25% of generator 3 load factor above a 72% threshold. This difference indicates that the generator 3 load factor is not as good as generators 1 and 4's load factors, despite being among the most utilized on the power grid. Further study must investigate the power grid generator ratings mixture that is best for fuel consumption. Our current experimental design is not set up to vary generator rating combinations.

4.2.5 Other Model Insights

We now analyze the model temperature behavior within the shelters for additional insights. Individual thermostats control the shelters' temperatures, and the optimization model keeps all the shelters within the specified limit except for the four cases in which RH-PFK fails to find a feasible solution. Ordinarily, we expect the temperature variation to be narrow or cluster since the model's objective is to minimize fuel usage by keeping the temperature within limits. However, the thermostat in shelter 9 keeps the temperature much lower than those of other shelters, and shelters 5 and 6 are kept much warmer than the others. Figures 4.17 and 4.18 display smoothed results. Smoothing the temperature across 164 excursions for RH-PFK, and 161 excursions for RH-U, makes overall trends visible that are not necessarily evident from the raw data. For instance, we clearly see that shelters 1–4 and 7 are similar and slightly warmer than shelter 8. A closer look at the raw data reveals that shelter 9 has the lowest temperature in approximately half of the time steps across the entire

Gen1Load_ON_PFK

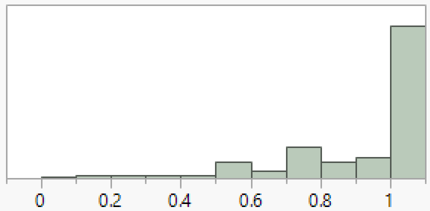

Quantiles

100.0%	maximum	1
99.5%		1
97.5%		1
90.0%		1
75.0%	quartile	1
50.0%	median	1
25.0%	quartile	0.827175
10.0%		0.66325
2.5%		0.5
0.5%		0.1
0.0%	minimum	0

Summary Statistics

Mean	0.9011298
Std Dev	0.1722293
Std Err Mean	0.0014783
Upper 95% Mean	0.9040274
Lower 95% Mean	0.8982322
N	13574

Gen2Load_ON_PFK

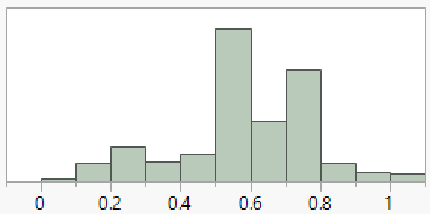

Quantiles

100.0%	maximum	1
99.5%		1
97.5%		0.92337
90.0%		0.75176
75.0%	quartile	0.74555
50.0%	median	0.5615
25.0%	quartile	0.5
10.0%		0.2602
2.5%		0.1
0.5%		0.1
0.0%	minimum	0

Summary Statistics

Mean	0.5713594
Std Dev	0.1914531
Std Err Mean	0.0021566
Upper 95% Mean	0.5755869
Lower 95% Mean	0.5671319
N	7881

Gen3Load_ON_PFK

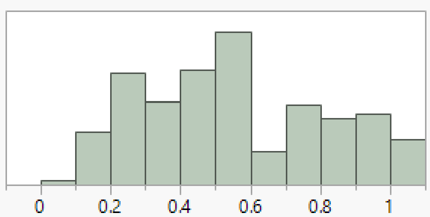

Quantiles

100.0%	maximum	1
99.5%		1
97.5%		1
90.0%		0.9575
75.0%	quartile	0.759025
50.0%	median	0.5
25.0%	quartile	0.3471
10.0%		0.25
2.5%		0.1
0.5%		0.1
0.0%	minimum	0

Summary Statistics

Mean	0.5462663
Std Dev	0.2614638
Std Err Mean	0.0025041
Upper 95% Mean	0.5511749
Lower 95% Mean	0.5413577
N	10902

Gen4Load_ON_PFK

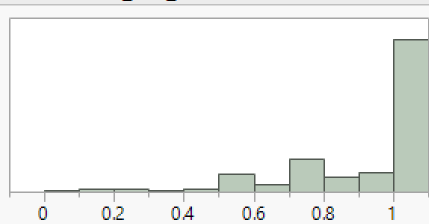

Quantiles

100.0%	maximum	1
99.5%		1
97.5%		1
90.0%		1
75.0%	quartile	1
50.0%	median	1
25.0%	quartile	0.8066
10.0%		0.63474
2.5%		0.49138
0.5%		0.1
0.0%	minimum	0

Summary Statistics

Mean	0.8963135
Std Dev	0.17794
Std Err Mean	0.0015313
Upper 95% Mean	0.899315
Lower 95% Mean	0.8933119
N	13503

Figure 4.15. Experiment II Distribution of Generators' Load during Operation, RH-PFK.

Gen1Load_ON_U

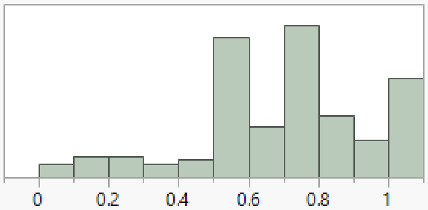

Quantiles

100.0%	maximum	1
99.5%		1
97.5%		1
90.0%		1
75.0%	quartile	0.8648
50.0%	median	0.75
25.0%	quartile	0.5
10.0%		0.3953
2.5%		0.1
0.5%		0
0.0%	minimum	0

Summary Statistics

Mean	0.6847218
Std Dev	0.243023
Std Err Mean	0.0020158
Upper 95% Mean	0.6886731
Lower 95% Mean	0.6807705
N	14534

Gen2Load_ON_U

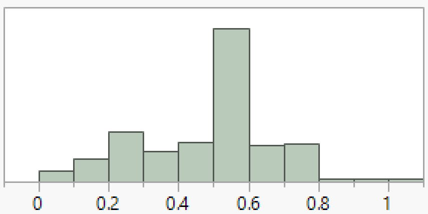

Quantiles

100.0%	maximum	1
99.5%		1
97.5%		0.75
90.0%		0.72528
75.0%	quartile	0.5624
50.0%	median	0.5
25.0%	quartile	0.356
10.0%		0.25
2.5%		0.1
0.5%		0
0.0%	minimum	0

Summary Statistics

Mean	0.468807
Std Dev	0.1832292
Std Err Mean	0.0020839
Upper 95% Mean	0.4728921
Lower 95% Mean	0.464722
N	7731

Gen3Load_ON_U

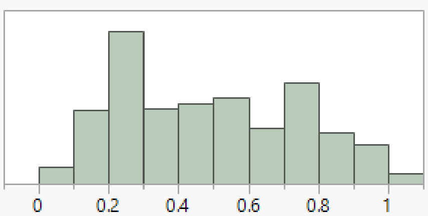

Quantiles

100.0%	maximum	1
99.5%		1
97.5%		0.970285
90.0%		0.8465
75.0%	quartile	0.724025
50.0%	median	0.45835
25.0%	quartile	0.25
10.0%		0.16856
2.5%		0.1
0.5%		0
0.0%	minimum	0

Summary Statistics

Mean	0.4830264
Std Dev	0.2565881
Std Err Mean	0.0021019
Upper 95% Mean	0.4871464
Lower 95% Mean	0.4789064
N	14902

Gen4Load_ON_U

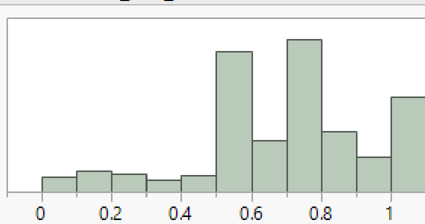

Quantiles

100.0%	maximum	1
99.5%		1
97.5%		1
90.0%		1
75.0%	quartile	0.8552
50.0%	median	0.75
25.0%	quartile	0.5
10.0%		0.3851
2.5%		0.1
0.5%		0
0.0%	minimum	0

Summary Statistics

Mean	0.6800836
Std Dev	0.2454627
Std Err Mean	0.0020349
Upper 95% Mean	0.6840722
Lower 95% Mean	0.676095
N	14551

Figure 4.16. Experiment II Distribution of Generators' Load during Operation, RH-U.

experiment, and has the lowest average temperature in every single excursion. We observe this behavior in both model variants as well as in both two experiments. As Sprague notes, the optimization model frequently maintains shelters below their maximum temperature thresholds for long periods of time. This occurs when a generator must run in order to cool other shelters, but its entire capacity is not needed for those shelters. Rather than run the generator at a low (inefficient) load factor for a long period of time, the model chooses to run the generator at a high load factor for a short period of time, essentially "getting ahead" in terms of cooling one of the shelters. Such behavior is a natural outcome of a prescriptive optimization approach, but can be difficult to encode in a simple policy such as the LGCY model.

One aspect Sprague does not mention is the apparent relationship between the shelter characteristics and the average temperature. He states that "the optimally scheduled ECUs elects to operate exclusively near the upper, more fuel efficient, limit." However, our results indicate that this phenomenon may be at least somewhat dependent on shelter characteristics, since different shelters exhibit different temperature behaviors. For instance, shelters 8 and 9 have different thermal intercept characteristics than the rest of the shelters and tend to be cooler, while shelters 5 and 6 have lower-powered ECUs and tend to be hotter than the other shelters. Further research could investigate the cause and degree of consistency of this behavior among varying grid setups.

Also, we compare the behavior of the cumulative total fuel consumption for the two model variants and the two experiments. This plot represents the averages of the 164 completed runs from experiment I, and the 161 completed runs from experiment II. The plot of cumulative fuel consumption over time shows a linear relationship with a steeper slope for both model variants in the first experiment. However, the relationship is nonlinear in the second experiment, with the slope decreasing between time 100 and time 200. This change corresponds to the period of day with higher renewable energy production — peaking between time step 120 and time step 180, depending on the design point — therefore, lower generator usage and subsequently lower fuel consumption. Figure 4.19 displays the results.

In addition, we examine the fuel consumption variation for five replications across the 33 design points in experiment II. Figure 4.20 reflects fuel consumption variation for different

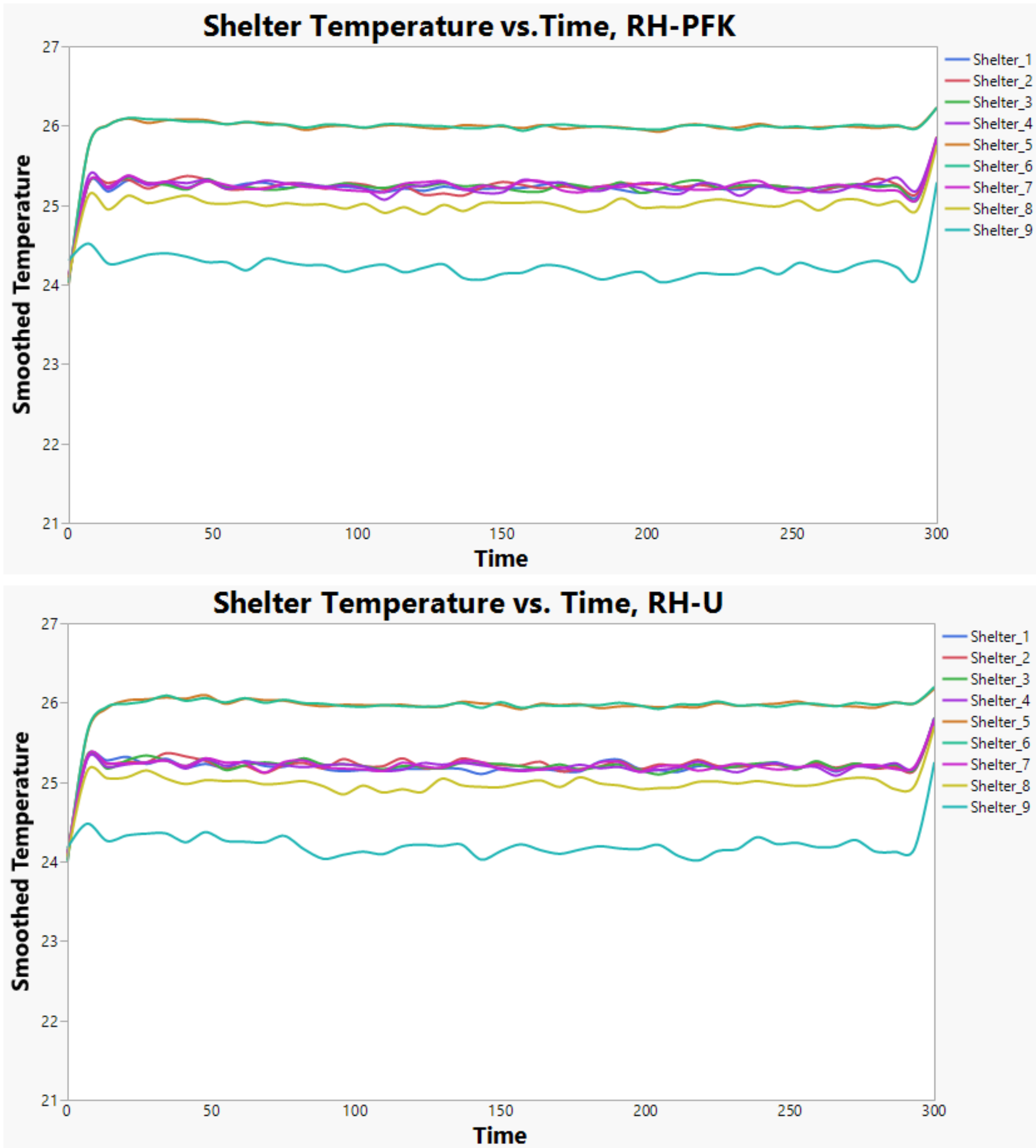

Figure 4.17. Experiment I Smoothed Temperature Variation, RH-PFK and RH-U.

times of day and different days of the week as represented by the factor combinations of the design points. This figure helps identify those times or days, as well as factor variation combinations, responsible for the spike in fuel consumption so that decision makers can better manage resource allocation accordingly. This insight represents another advantage of employing a structured DOE approach with multiple replications across multiple design points to gain insight.

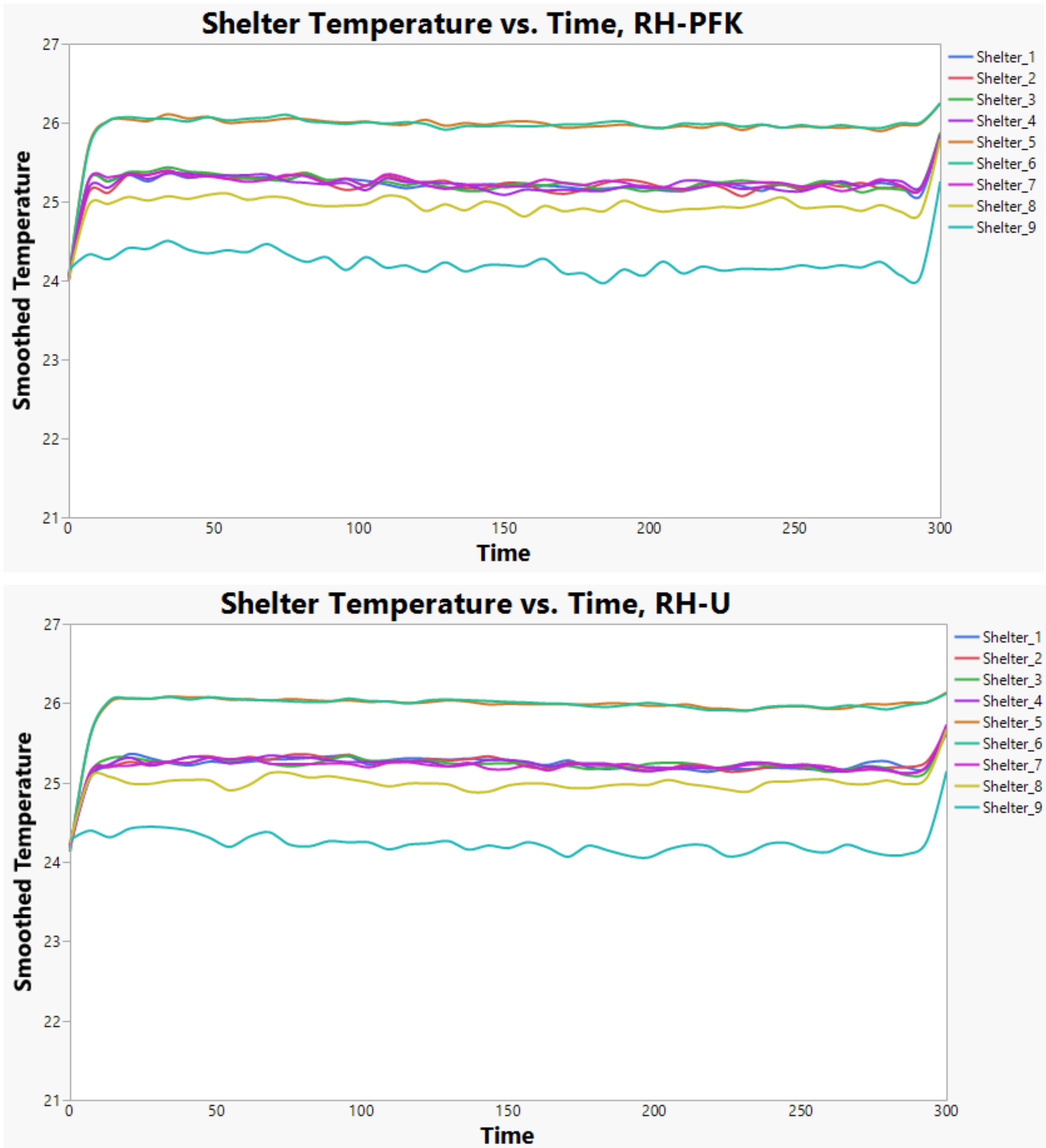

Figure 4.18. Experiment II Smoothed Temperature Variation, RH-PFK and RH-U.

Figure 4.21 displays the mean relative efficiency of five replications and 33 design points on the left, and on the right shows the same display broken down by design point. The data for this comparison comes from experiment II, as it uses a more realistic reflection of actual demand and production patterns. This figure presents the times and days as well as factor combinations of when one model variant performs better than the other on fuel consumption. Although RH-PFK performs better on average across all design points, in

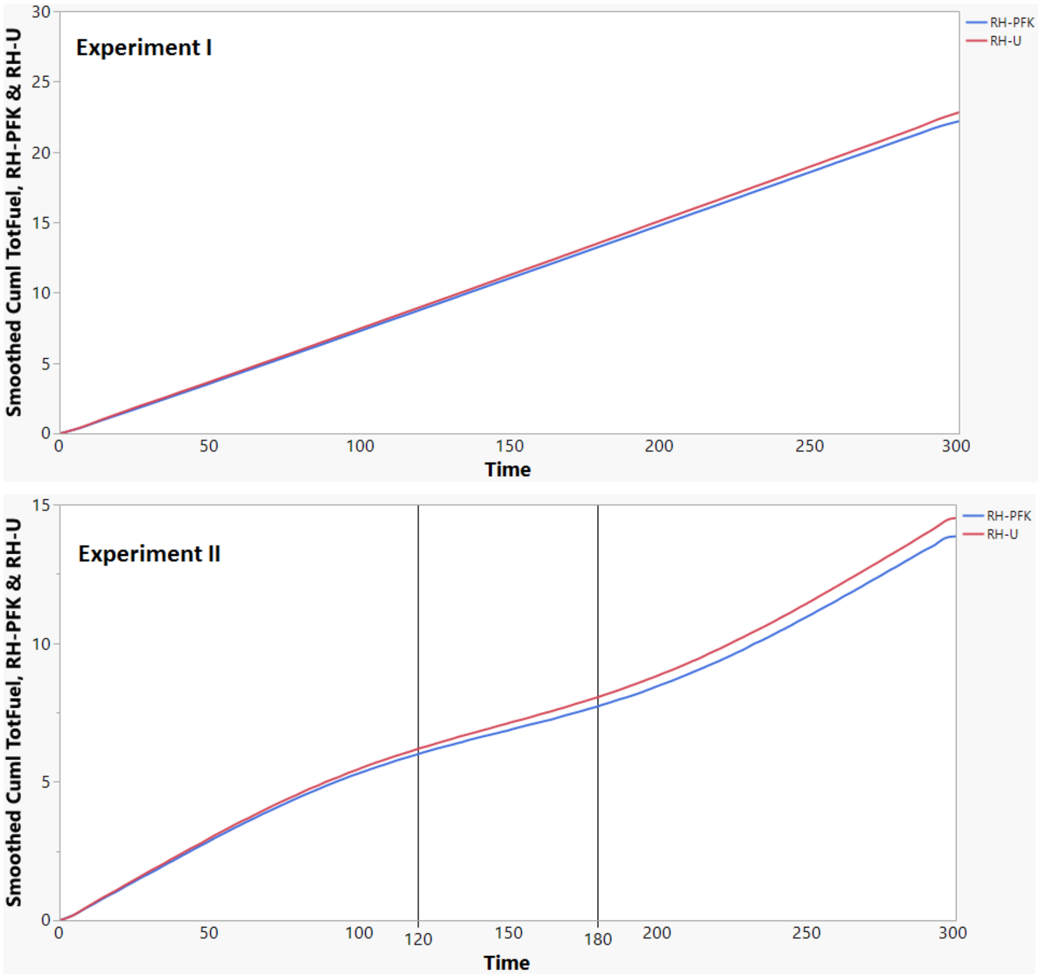

Figure 4.19. Cumulative Total Fuel Consumption, RH-PFK vs. RH-U

some factor combinations on certain times or days, the RH-U performs better. This can be due to the particular values of the random data (i.e., "luck"), or an artifact of the rolling horizon implementation, or due to the optimality tolerances used in the model; in any case, the absolute differences in performance are small in early time steps. However, as the time horizon progresses, RH-PFK starts to do better, as expected. A closer look at the plot on the right shows design point 6 exhibits wider variation than the others. This is the same design point that failed to solve to completion in some instances, indicating that it represents a particularly challenging problem instance. Therefore, uncertainty of future demand, renewable production, or heat transfer increases fuel consumption, but not by a significant margin, as the relative efficiency plot shows. How much a power buffer must

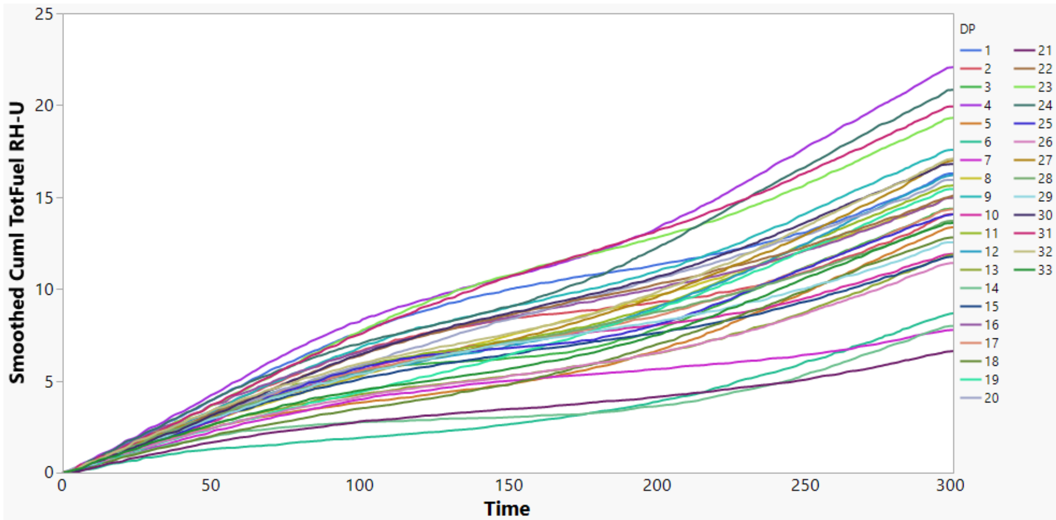

Figure 4.20. Cumulative Total Fuel Consumption Variation by Design Point, RH-U

be present for the grid to withstand these uncertainties and improve the power grid system resilience is a trade-off decision to be made.

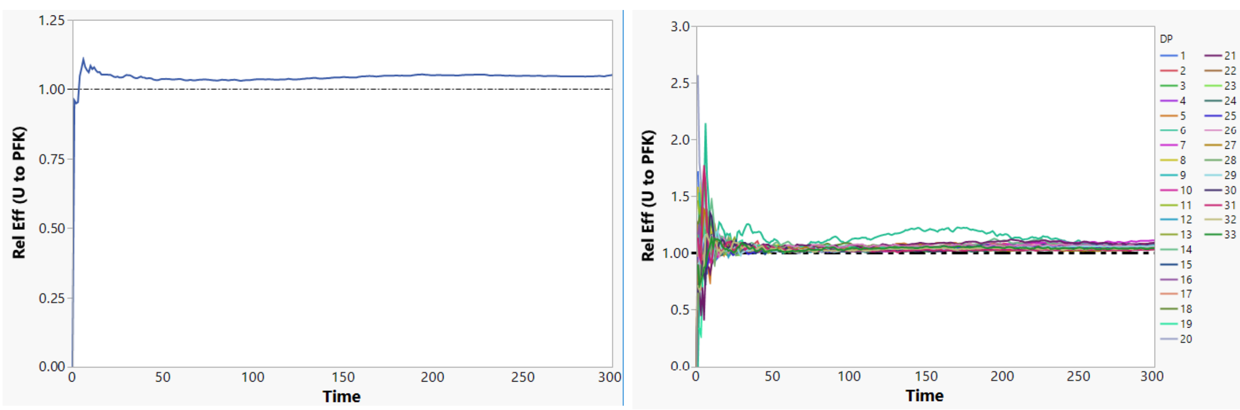

Figure 4.21. Relative Efficiency, RH-U

4.3 Analysis Summary

We have investigated uncertain factors influencing cumulative total fuel consumption by analyzing the DOE of a power grid optimization model. Introducing realistic energy production and unscheduled demand data into experiment II uncovers additional insights that apply in real life situations. Also, our analysis provides useful insights on the generators'

behavior, the temperature's behavior, and the cumulative total fuel consumption in the model.

CHAPTER 5:
Conclusions and Future Work

5.1 Conclusion

This thesis investigates uncertain factors influencing optimal scheduling of time-shiftable electric loads under uncertainty to gain insights and to support the future development of a robust optimization for scheduling such loads. Our analysis of Sprague's model [1] reveals the uncertain factors contributing to fuel consumption, as well as provides useful insights on the generators' behavior in the model. We identify the heat transfer intercept mean of the expeditionary shelters as the dominant factor contributing to fuel consumption in the model, among the parameters we consider and the magnitude of the uncertainty we investigate. The implication is that structures' or shelters' characteristics play an important role in how much cooling must maintain the shelter's internal temperature within acceptable limits. Greater cooling requirements directly translate into greater fuel consumption. Therefore, choosing the right types of shelter when establishing FOBs is a good way to reduce fuel consumption.

The composition of the energy grid power production system affects the results of the identified factor(s) influencing generator fuel consumption. The majority of the power production in Sprague's model is from the generator, as employed in current practice within the DOD. However, the outcome varies when we increase the renewable power production and unscheduled demand, and then vary them with other uncertain parameters in our DOE analysis. Our implementation of these changes in experiment II produces different factors that influence fuel consumption. This result implies decisions on setting up FOBs must be preceded by a careful analysis and determination of optimal energy production composition for the power grid, as well as a realistic estimation of the unscheduled demand requirements and renewable energy production. Such practices ensure the right mix of energy production capacity prior to establishing FOBs so as to minimize power grid fuel consumption.

Resource management of limited DOD assets could be improved through insights from the analysis of the generators' behavior. For example, some generators ran at low load factors much of the time, even when they were optimally scheduled to run. Although power

demand requirements could increase with little to no notice, our analysis shows improvement possibilities, especially with the knowledge of future requirements. Both model variants and both experiments illustrate that the power grid requires one or two generators most of the time and rarely requires all four generators at once. Running more generators than necessary often leads to a low load factor that reduces fuel efficiency. We conclude that a structured DOE that investigates power grid generators' rating combinations, in addition to the factors in this study, is required to ensure the right mix of generators is chosen for the power grid.

Analysis of the temperature variations within the expeditionary shelters and the cumulative total fuel consumption yields additional insights. The cumulative total fuel consumption analysis suggests that uncertainty in unscheduled demand might not lead to a huge drop in relative efficiency afterwards. Decision makers need to examine how much to invest in a power production buffer for the power grid to deal with uncertainty and increase the system's resilience. Our analysis in this study reveals uncertainty does not harm the power grid too much.

While optimal scheduling of time-shiftable electrical loads has already been shown to reduce generator fuel consumption, our analysis of Sprague's optimization model provides more insights on additional improvements. These opportunities could be pursued in different ways, ranging from improving structures and shelter characteristics, to changing power production composition on the grid.

5.2 Future Work Recommendations

Our study reveals fuel consumption of conventional fossil fuel generators could be reduced with proper planning and analysis of optimal scheduling of time-shiftable loads. Opportunities exist to improve and continue this research work.

5.2.1 Robust Optimization Model Development

Implementation of robustness into Sprague's model could further reduce generators' fuel consumption, and should be investigated. We performed a preliminary study of developing a robust version of Sprague's optimization model and found that the computation time for a robust model is quite high. Future work could investigate this further.

As mentioned earlier, some of our findings may support the development of a robust optimization model by focusing attention on the aspects of the model and environment that make a difference to the solution quality under uncertainty, and the solution timeliness.

5.2.2 Robustness Investigation via Designed Experiments

We obtained useful insights from our DOE and an analysis of Sprague's model. The inclusion of experiment II in our analysis offered more insights than we could have obtained with only the baseline input data. Other factors, including the power generation capacity mix, temperature limit ranges, and so on could be varied to obtain more insights. Future work could select other factors to vary, as well as study the behavior of other responses that may be of interest for practical applications.

Also, our analysis provides insights into the behavior of the model; we recommend future work directly compare a robust optimization formulation of the model to the DOE approach for assessing robustness.

5.3 Final Thoughts

This study comes from a desire to improve U.S. military energy use on the battlefield. The cost associated with too much energy use goes beyond monetary resources; lives are lost, and the budget for future capabilities is diminished. This thesis provides useful insights on how to reduce power grid energy consumption by using a powerful combination of an optimization model and DOE analysis. Ultimately, the U.S. military expeditionary power grid system should be resilient and self-sustaining for our assigned missions around the world.

THIS PAGE INTENTIONALLY LEFT BLANK

List of References

[1] J. Sprague, "Optimal scheduling of time-shiftable electric loads in expeditionary power grids," Master's thesis, Operations Research Dept., Naval Postgraduate School, Monterey, CA, Sep. 2015.

[2] J. Warner and P. Singer. (2008). "Fueling the "balance" a defense energy strategy primer". Brookings Institution. [Online]. Available: http://www.brookings.edu/~/media/research/files/papers/2009/8/defense-strategy-singer/08_defense_strategy_singer.pdf

[3] M. Schwartz, K. Blakely, and R. O'Rourke. (2012, June). "Department of Defense energy initiatives: Background and issues for Congress". Congressional Research Service, Washington, DC. [Online]. Available: https://www.fas.org/sgp/crs/natsec/R42558.pdf

[4] Office of the Assistant Secretary of Defense for Energy, Installations, and Environment. (2016). "About operational energy". [Online]. Available: http://www.acq.osd.mil/eie/OE/OE_index.html

[5] U.S. Energy Information Administration, "Annual energy review 2011," U.S. Department of Energy, Washington DC., U.S. Department of Energy, Washington DC., Report, 2012.

[6] Office of the Assistant Secretary of Defense (Energy, Installations and Environment), "Department of Defense 2016 operational energy strategy," Department of Defense, Washington, DC, Report, 2016.

[7] S. Burke, "Statements submitted to the Subcommittee on Readiness and Management Support, Senate Armed Services Committee," Assistant Secretary of Defense for Operational Energy Plans and Programs, 2014.

[8] Office of the Under Secretary of Defense (Acquisition, Technology, and Logistics), "2007 Defense Science Board (DSB) task force on DOD energy strategy," Department of Defense, Washington DC, Final Report, 2008.

[9] P. Bulanow, P. Tabler, and S. Charchan, "Expeditionary energy assessment environmental control unit alternatives study," U.S. Marine Corps Expeditionary Energy Office, Quantico, VA, Final Report, 2011.

[10] S. Burke and L. Hayward. (2015). "How DOD is cutting oil consumption to create a better military". [Online]. Available: http://energyfuse.org/sharon-burke-how-

cutting-military-oil-consumption-helps-create-a-leaner-more-powerful-department-of-defense/

[11] Assistant Secretary of Defense for Operational Energy, Plans and Programs, “Energy for the warfighter: operational energy strategy,” Department of Defense, Washington, DC, Final Report, 2011.

[12] Marine Energy Assessment Team, “Afghanistan Assessment Outbrief,” United States Marine Corps, Headquarters Marine Corps, Report, 2010. Available: http://www.dtic.mil/ndia/2010MCexpeditionary/moore.pdf

[13] C. F. Wald and T. Captain, “Energy security – America’s best defense: a study conducted by Deloitte Development LLC, of energy use during wartime,” Deloitte Development LLC, Tech. Rep., 2009.

[14] Marine Corps Systems Command, “Expeditionary Power Systems – National Defense Industrial Association brief,” Quantico, VA, Tech. Rep., 2016. Available: http://www.ndia.org/Divisions/Divisions/Manufacturing/Documents/USMC20Power20and20Energy.pdf

[15] Leonardo Energy, “Electric load management in industry,” International Union for Electricity Applications (UIE), Report, 2009. Available: http://www.uie.org/sites/default/files/generated/files/pages/LoadManagement.pdf

[16] R. Kelly, “Optimizing gas generator efficiency in a forward operating base using an energy management system,” Master’s thesis, Electrical Engineering Dept., Naval Postgraduate School, Monterey, CA, June 2013.

[17] T. Mansfield, H. Place and D. Smith, “Hybrid tactical power system,” Electrical Engineering Dept., United States Military Academy, West Point, New York, Undergraduate Study, April 2015. Available: http://www.ncurproceedings.org/ojs/index.php/NCUR2015/article/viewFile/1466/728

[18] H. Bouaicha, “Optimal day-ahead scheduling of a hybrid electric grid using weather forecasts,” Master’s thesis, Operations Research Dept., Naval Postgraduate School, Monterey, CA, Dec. 2013.

[19] N. A. Ulmer, “Optimizing microgrid architecture on department of defense installations,” Master’s thesis, Operations Research Dept., Naval Postgraduate School, Monterey, CA, Sep. 2014.

[20] U.S. Army Communications-Electronics Research, Development and Engineering Center. "Tactical and deployed power". [Online]. Available: http://www.cerdec.army.mil/inside_cerdec/core_technology/tactical_and_deployed_power/

[21] SunDanzer DC-powered refrigeration. (2016). "Direct current air cooler, DCAC". [Online]. Available: http://www.sundanzer.com/product/dcac-air-cooler/

[22] P. Richard, “Department of Defense mobile electric power systems command brief,” Deputy Project Manager, DOD Project Manager Mobile Electric Power, Fort Belvoir, Virginia, Tech. Rep., Mar. 2009.

[23] E. Shaffer, “Innovative energy solutions for military applications,” Energy and Power Division, U.S. Army Research Laboratory, Adelphi, Maryland, Tech. Rep., Nov. 2014. Available: https://www.iesma.info/download/125/8(2)_shaffer.pdf

[24] *Operator and Field Maintenance Manual for Power Distribution Illumination Systems, Electrical (PDISE)*, TM 9-6150-226-13 ed., U.S. Army Headquarters, Washington, DC, Apr. 2012.

[25] R. A. Fisher, “The arrangement of field experiments,” *Journal of the Ministry of Agriculture of Great Britain*, vol. 33, pp. 503–513, 1926. Available: http://hdl.handle.net/2440/15191

[26] T. P. Speed, “Introduction to “The arrangement of field experiments" by R.A. Fisher,” University of California, Berkeley, California, Tech. Rep. 253, May 1990.

[27] S. M. Sanchez, T. W. Lucas, P. J. Sanchez, C. J. Nannini, and H. Wan, “Designs for large-scale simulation experiments, with applications to defense and homeland security,” in *Design and Analysis of Experiments: Special Designs and Applications*, vol. 3, K. Hinkelmann, Ed., 1st ed. New York: John Wiley & Sons, 2012, ch. 12, pp. 413–441.

[28] S. M. Sanchez and H. Wan, “Work smarter, not harder: A tutorial on designing and conducting simulation experiments,” in *Proceedings of the 2014 Winter Simulation Conference*, A. Tolk, S. Y. Diallo, O. Ryzhov, L. Yilmaz, S. Buckley, and J. A. Miller, Eds. Piscataway, NJ: Institute of Electrical and Electronic Engineers, Inc., 2014, pp. 1795–1809. Available: http://www.informs-sim.org/wsc15papers/187.pdf

[29] Simulation Experiments and Efficient Design (SEED) Center for Data Farming. Home page. [Online]. Available: http://harvest.nps.edu.

[30] M. J. Gardner, “Investigating the naval logistics role in humanitarian assistance activities,” Master’s thesis, Operations Research Dept., Naval Postgraduate School, Monterey, CA, March 2015.

[31] H. Li, “Improving the Taiwan military’s disaster relief response to typhoons,” Master’s thesis, Operations Research Dept., Naval Postgraduate School, Monterey, CA, June 2015.

[32] M. M. Morse, "Assessing the robustness of HOMER for Marine Corps expeditionary operations," Master's thesis, MOVES Institute, Naval Postgraduate School, Monterey, CA, March 2014.

[33] S. M. Sanchez, M. M. Morse, S. C. Upton, M. L. McDonald, and D. A. Nussbaum, "A robust design approach to cost estimation: solar energy for Marine Corps expeditionary operations," in *Proceedings of the 11th Annual Acquisition Research Symposium*, 2014, pp. 519–537. Available: http://www.acquisitionresearch.net/files/FY2014/NPS-AM-14-C11P22R01-075.pdf

[34] T. M. Cioppa and T. W. Lucas, "Efficient nearly orthogonal and space-filling Latin hypercubes," *Technometrics*, vol. 49, no. 1, pp. 45–55, 2007.

[35] SAS Institute Inc., "JMP Pro version 12.0.1," Cary, NC, 1989-2007, 2016.

Initial Distribution List

1. Defense Technical Information Center
   Ft. Belvoir, Virginia

2. Dudley Knox Library
   Naval Postgraduate School
   Monterey, California